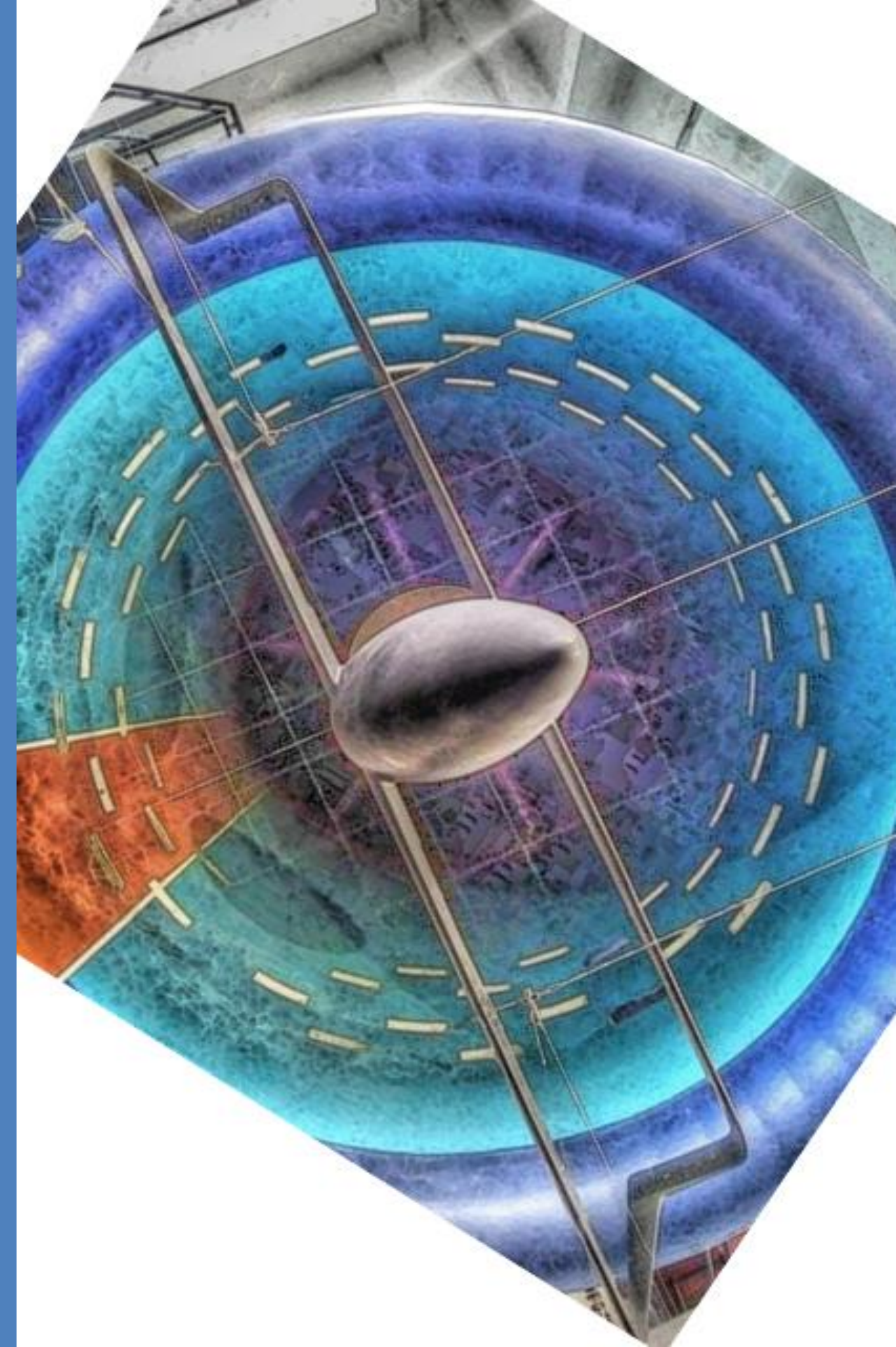


The science behind Aircraft Engineering

The Basics of Airfoil Design and
Airfoil-Airframe Integration



References

1. Aircraft design: a conceptual approach/Daniel P. Raymer. Published by American Institute of Aeronautics and Astronautics, Inc.
2. Darmofal, D., Drela, M., Uranga, A. Introduction to Aerodynamics: edX Course. - Massachusetts: MIT, 2016. – 515 p.
3. <http://airfoiltools.com/>
4. Anderson, John David. “Fundamentals of Aerodynamics.” (1984)
5. Gudmundsson, Snorri. “General Aviation Aircraft Design: Applied Methods and Procedures.” (2013)
6. Yang, Zifeng, Fred L. Haan, Hui Hu and Hongwei Ma. “An Experimental Investigation on the Flow Separation on a Low-Reynolds-Number Airfoil.” (2007)
7. Figures of Merit for Airfoil/Aircraft Design Integration by M.D. Maughmer and D.M. Somers. AIAA/AHS/ASEE Aircraft Design, Systems and Operations Meeting September 7-9, 1988/Atlanta, GA
8. Selig, Michael S. “Low Reynolds Number Airfoil Design Lecture Notes.”
9. Drela, Mark. “Low-Reynolds-number airfoil design for the M.I.T. Daedalus prototype- A case study.” Journal of Aircraft 25 (1988): 724-732.
10. Aircraft Performance and Design. J.D. Anderson. McGraw-Hill Publishing Company, Shoppenhangers Road, Maidenhead, Berks SL6 2QL, UK. 1999. 580pp
11. Li, Ji-chao, Xiaosong Du and Joaquim R.R.A. Martins. “Machine Learning in Aerodynamic Shape Optimization.” *ArXiv* abs/2202.07141 (2022)

Contents

Historical note

Airfoil geometry definition

Pressure coefficient

Properties of typical airfoils

Airfoil stall characteristics

Various approaches to airfoil design

Desired airfoil characteristics

Airfoil parameters and characteristics (direct analysis)

Airfoil inverse design

Machine Learning in Aerodynamic Shape Optimization

Airoil-Airframe integration

Quiz

What is an airfoil?

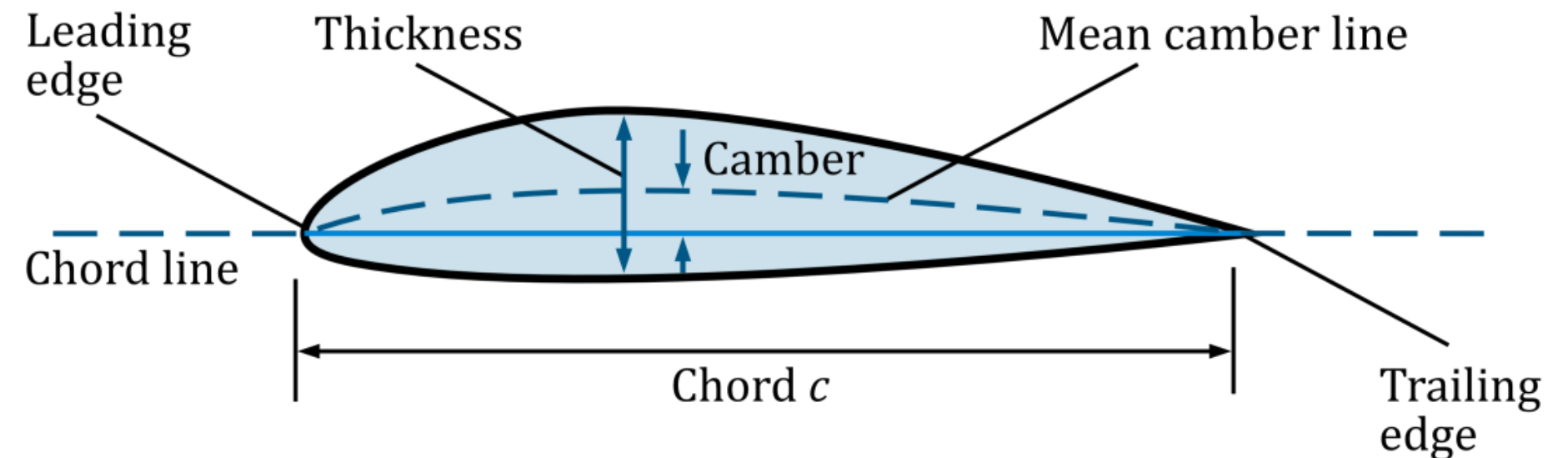
What types of airfoils do you know?

What is lift and how is it generated?

How the airfoil geometry and performance are related?

How does Reynolds number affects an airfoil's performance?

Airfoil geometry definition



Chord line: the chord line is a straight line connecting the leading and trailing edge of the airfoil.

Mean camber line: $z_c(x)$ is the mean camber line and is defined as the curve which is midway between the upper and lower surface measured normal to the mean camber line.

The maximum camber is the maximum value of $z_c(x)$.

Thickness distribution: $t(x)$ is the thickness distribution and is defined as the distance between the upper and lower surface measured normal to the mean camber line.

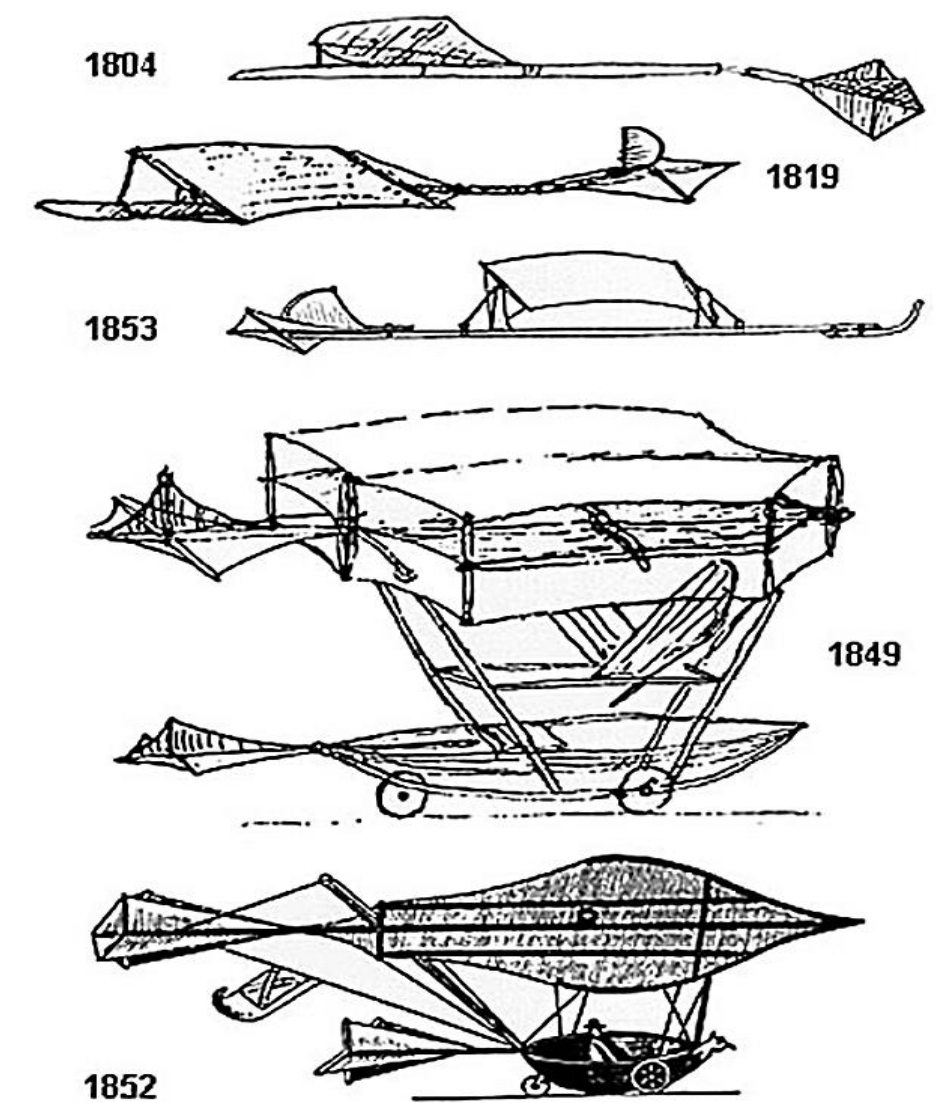
The maximum thickness is the maximum value of $t(x)$.

Historical note

1804

George Cayley

The first modern
configuration aircraft



Ref.: Aircraft Performance and Design by J.D. Anderson

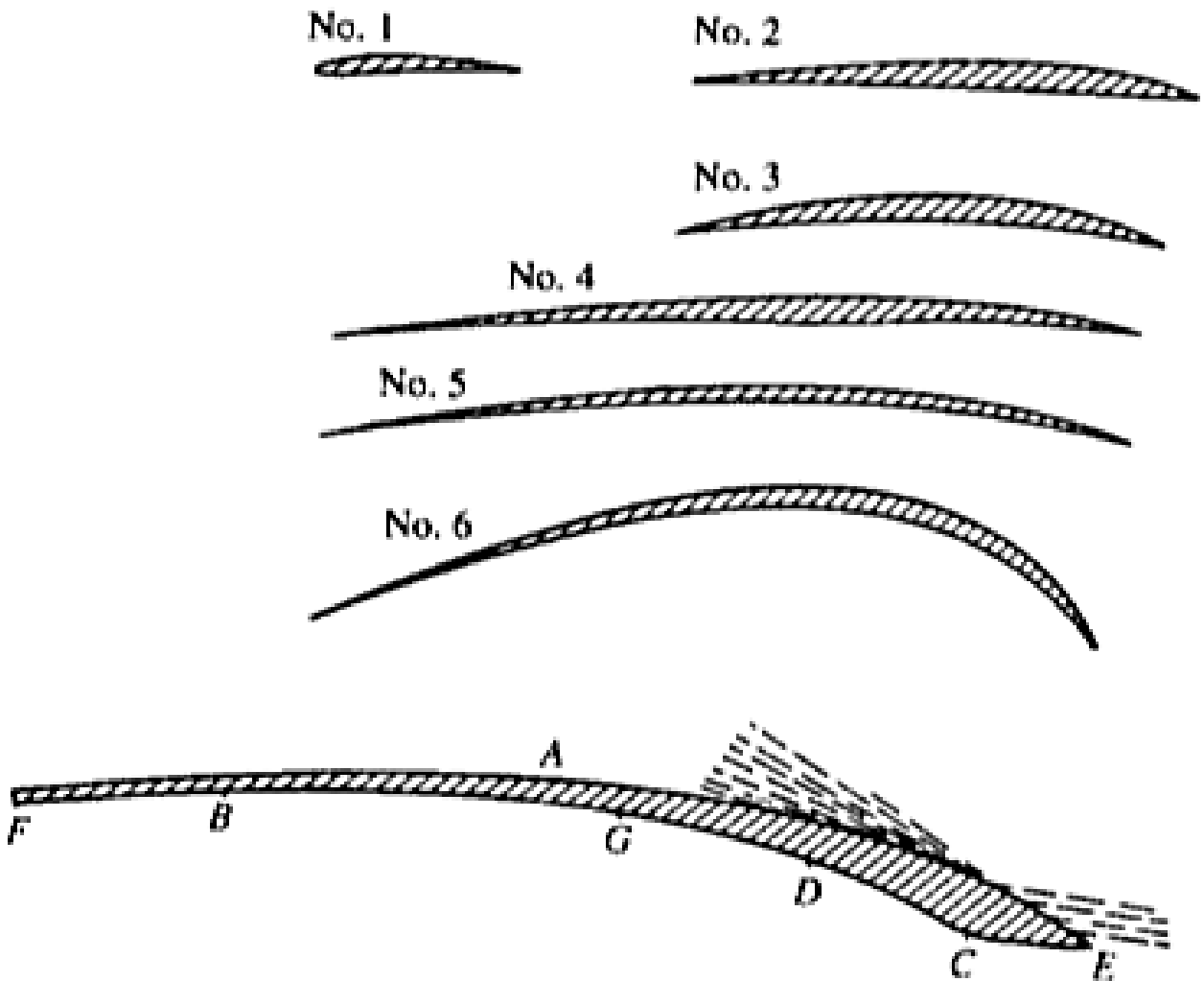
Historical note

1884

Horatio Phillips

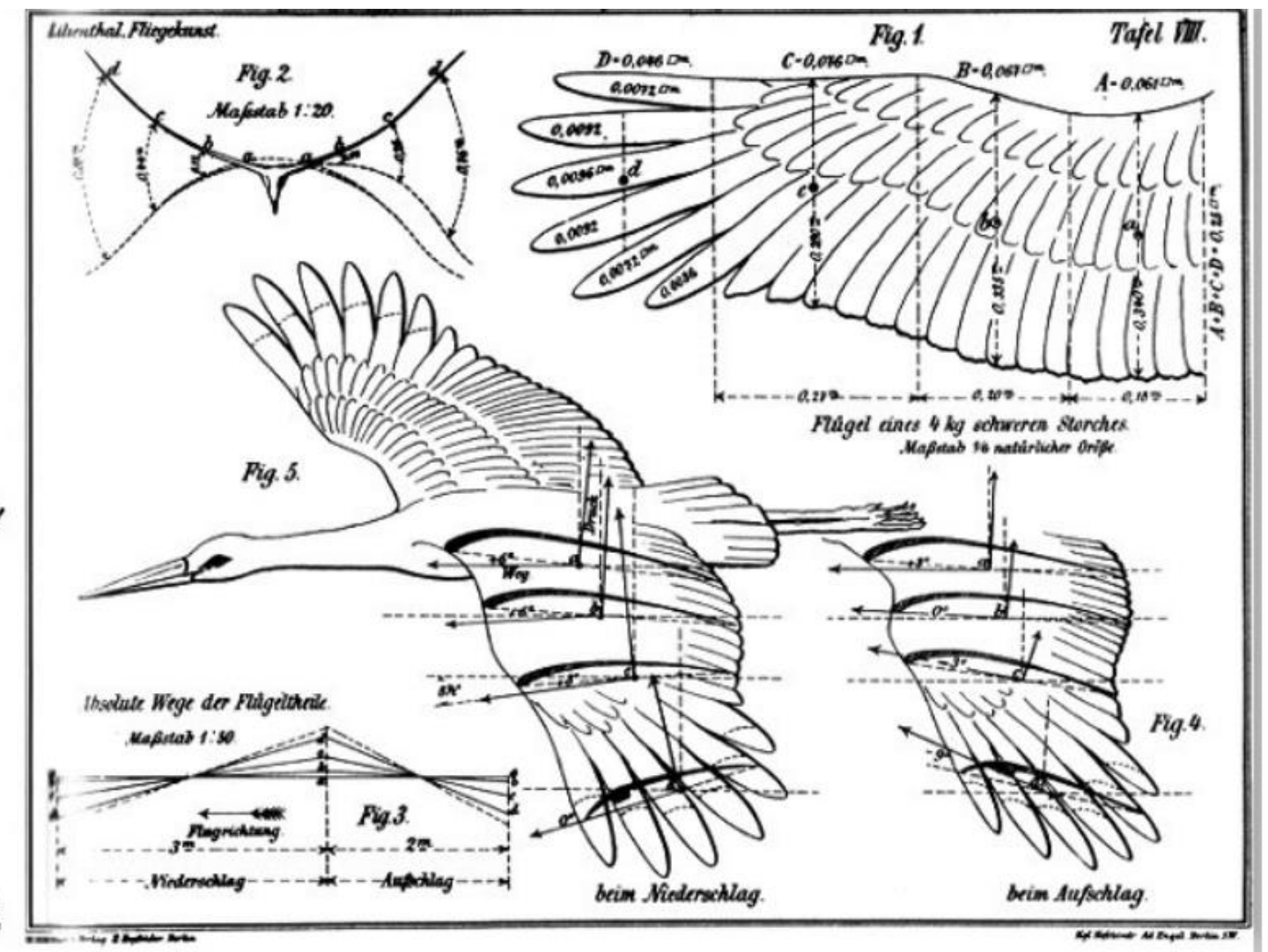
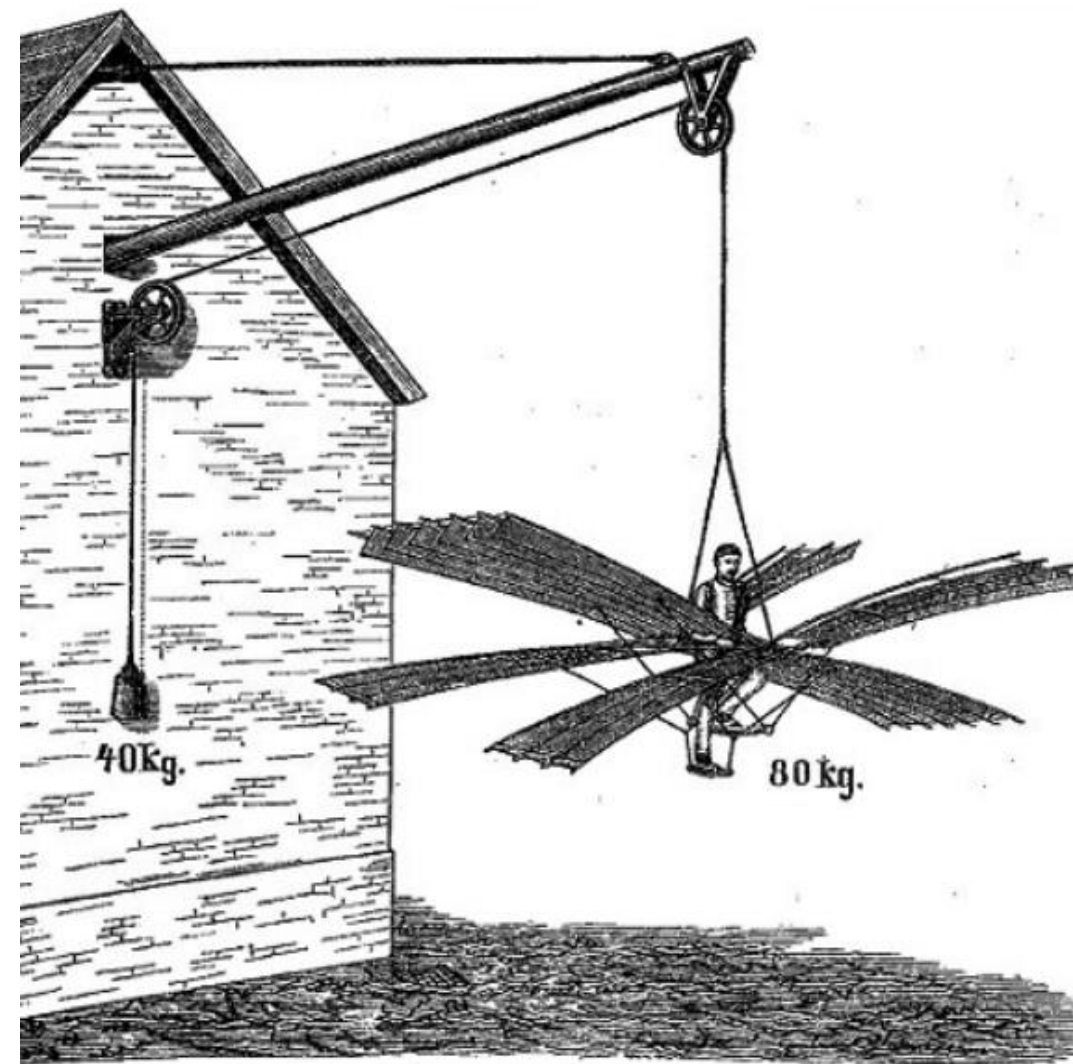
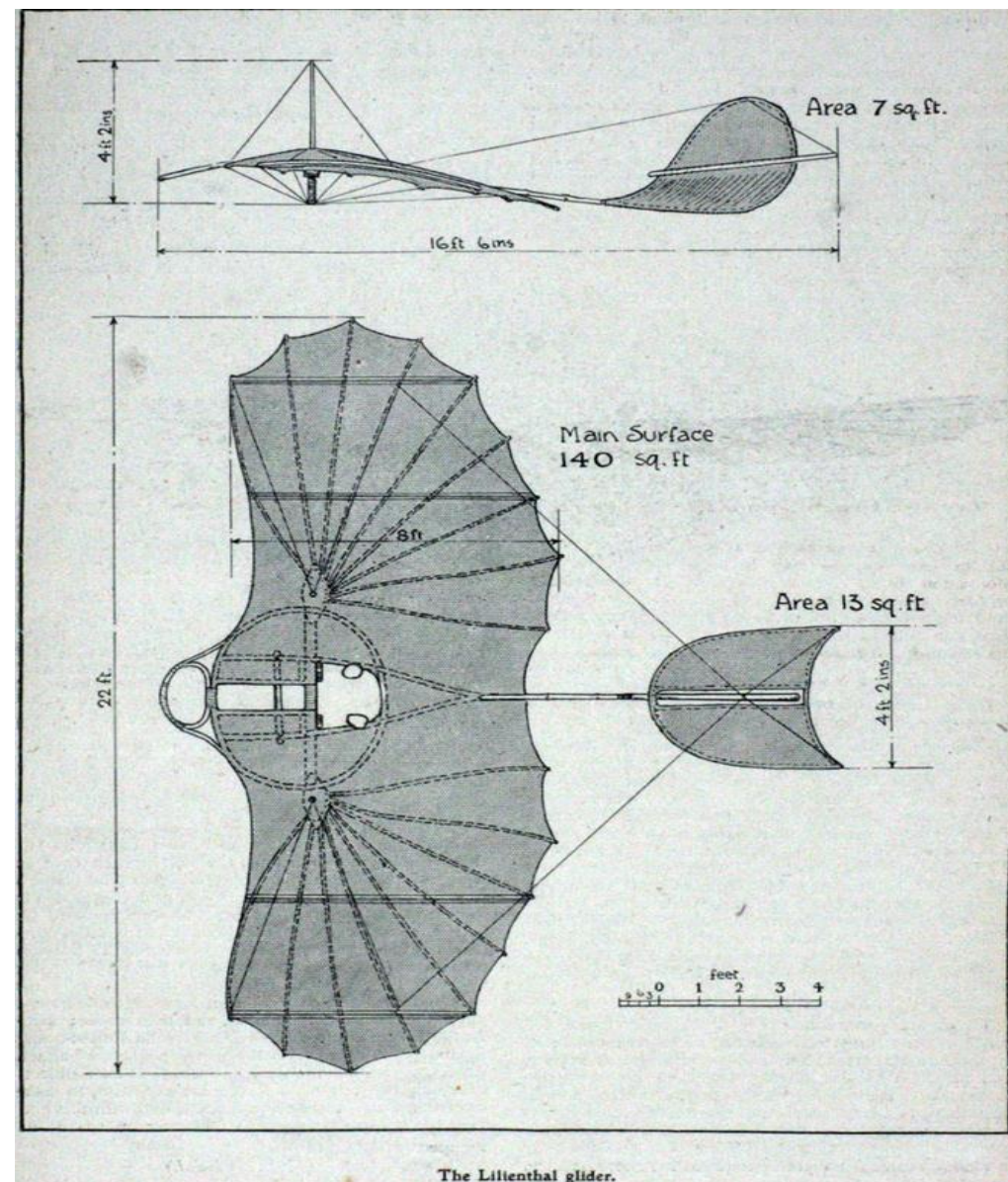
First wind tunnel experiments

Double-surface airfoil sections by Horatio Phillips. The six upper shapes were patented by Phillips in 1884; the lower airfoil was patented in 1891.



Historical note

Otto
Lilienthal Gliders

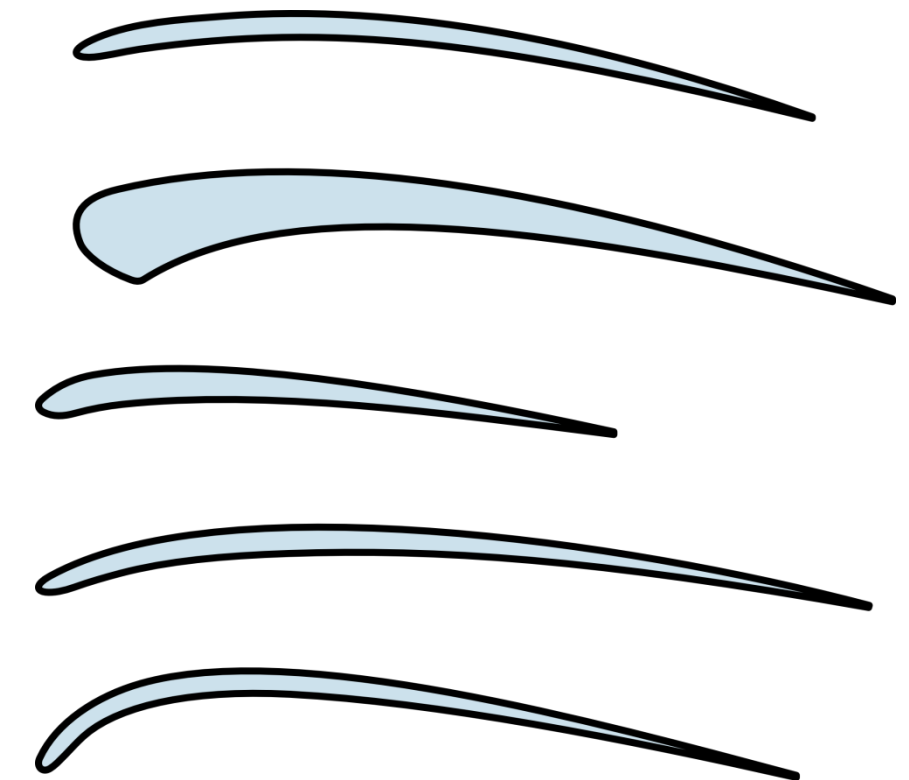
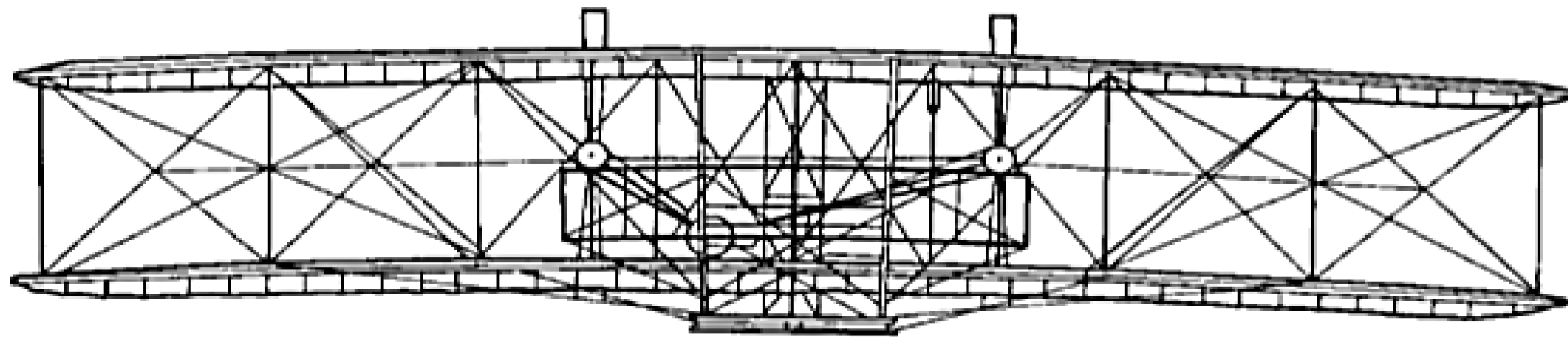


Historical note

1901-1903

The Wright
Brothers

Flyer



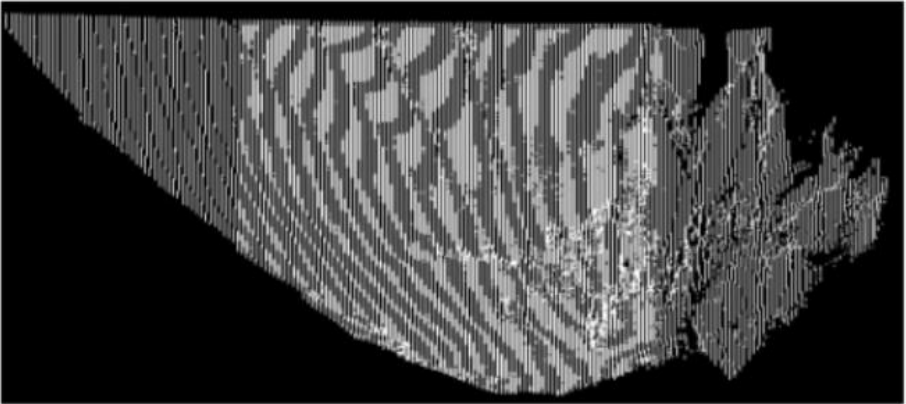
Bird wing airfoil

Table 1. Parameters of the bionic airfoil.

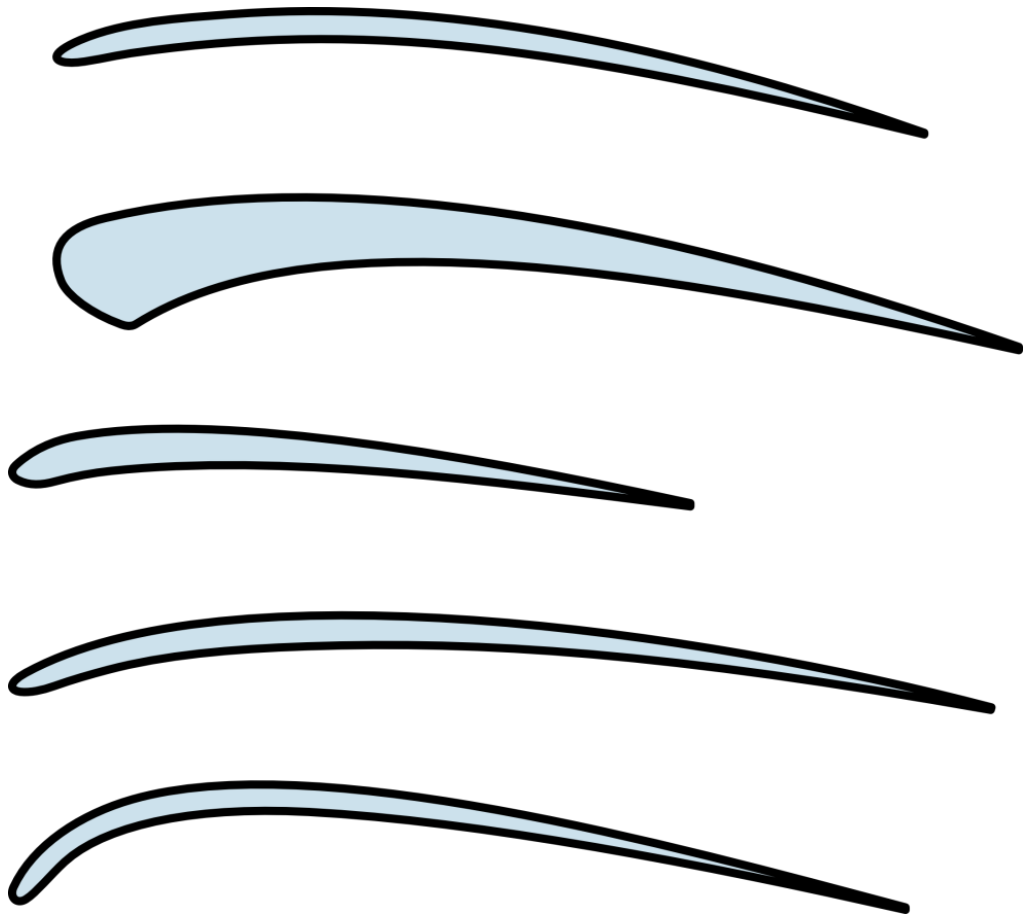
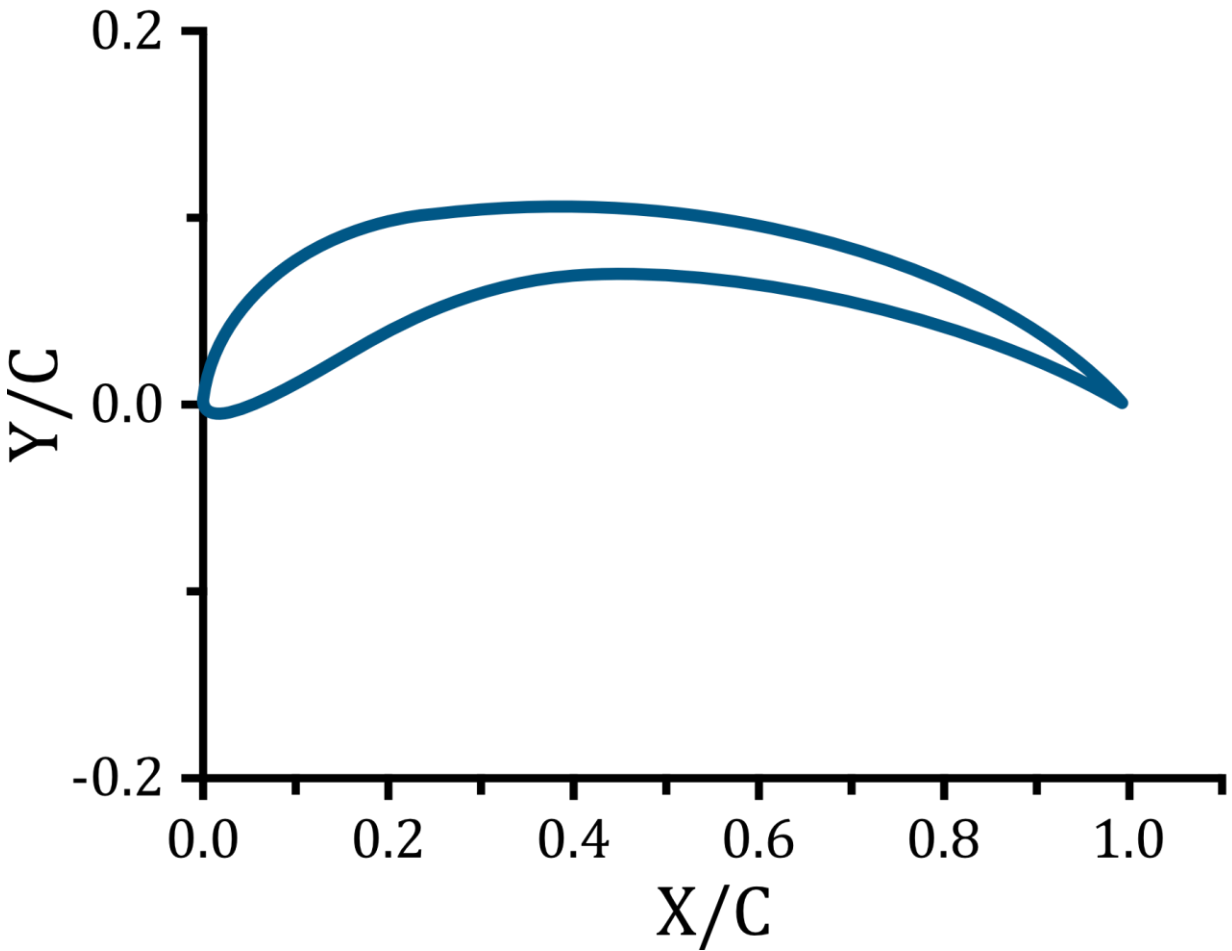
Variables	Values
Maximum thickness as a fraction of the chord (t)	$0.067 C$
Leading edge radius (r)	$0.0028 C$
Camber (f)	$0.0888 C$
Position of the maximum thickness (x_t/c)	9.1%
Position of the maximum camber (x_f/c)	45.5%



Swallow's wing



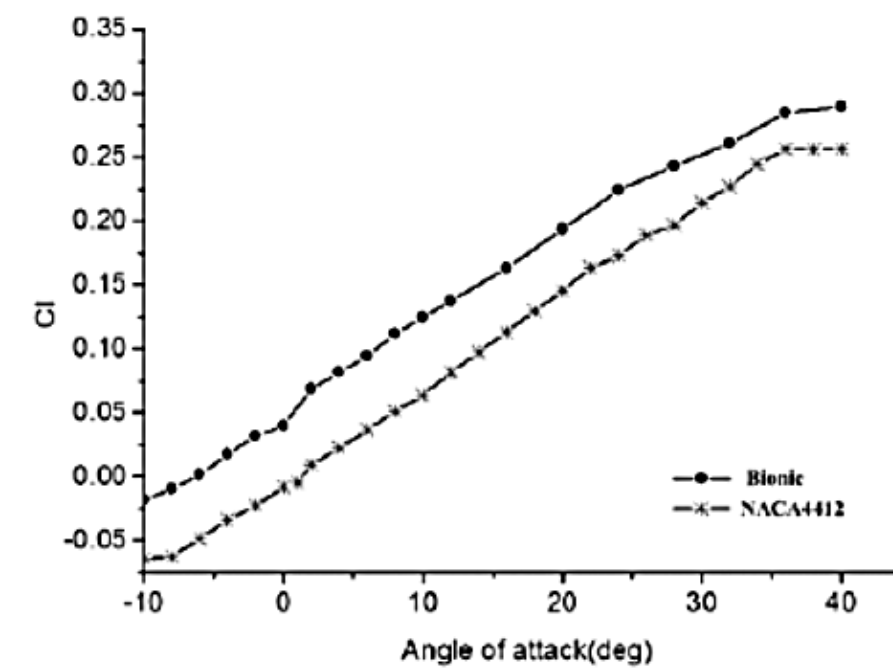
Data cloud of wing



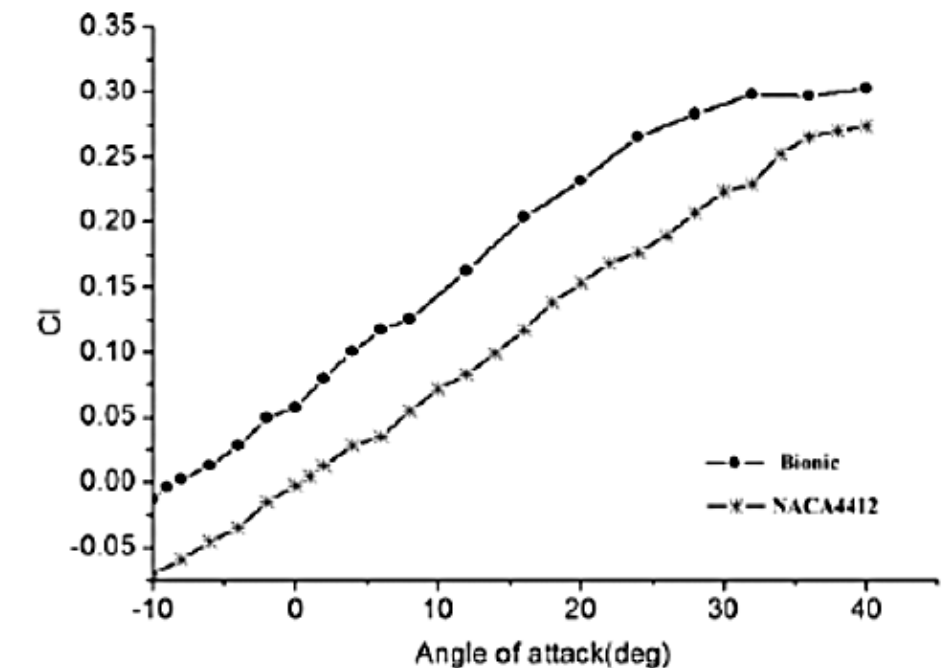
Ref.:
1. STUDY ON AERODYNAMIC PERFORMANCE OF THE BIONIC AIRFOIL BASED ON THE SWALLOW'S WING WEIJUN TIAN, QIAN CONG, YURONG LIU and LUQUAN REN
Key Laboratory of Bionic Engineering (Ministry of Education, China) Jilin University, Changchun, P. R. China Published 13 December 2013

Bird wing airfoil

Lift coefficient curves for standard airfoil (NACA4412) and bionic airfoil

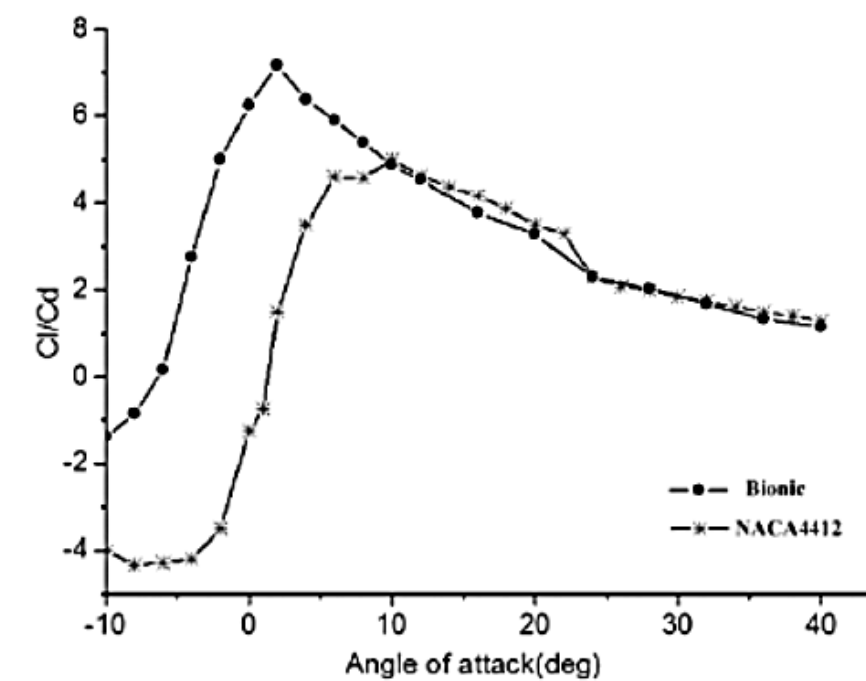


(a) 10 m/s

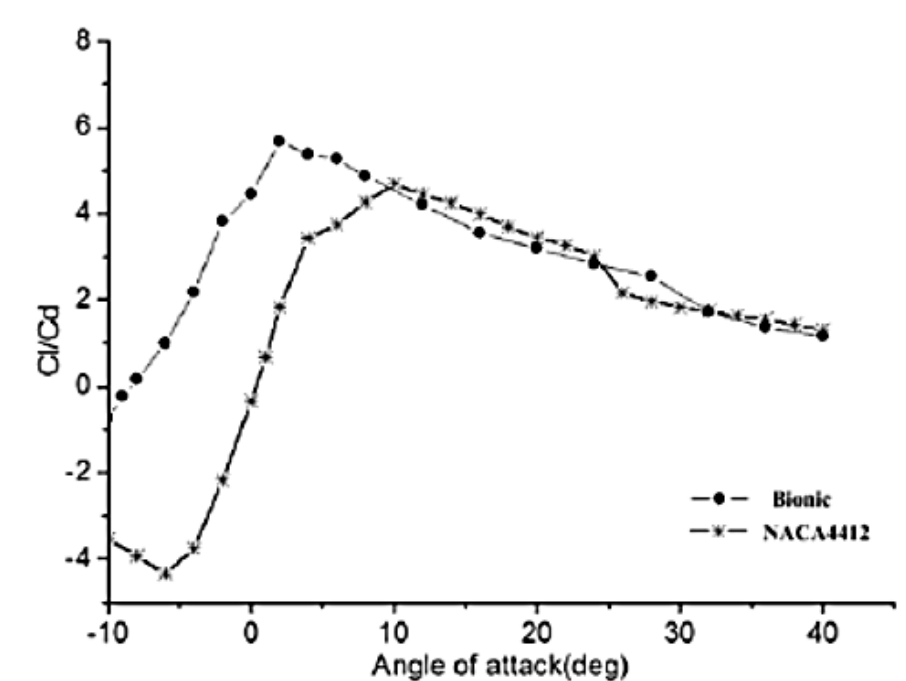


(b) 11.4 m/s

Lift-to-drag ratio curves for standard airfoil (NACA4412) and bionic airfoil

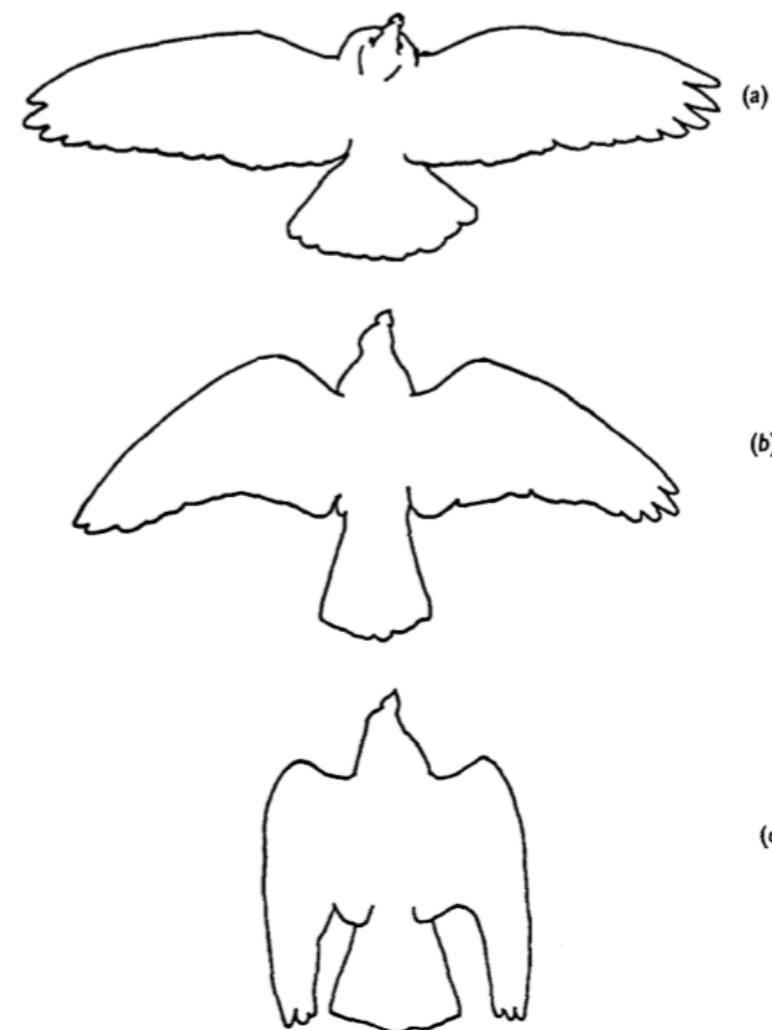


(a) 10 m/s

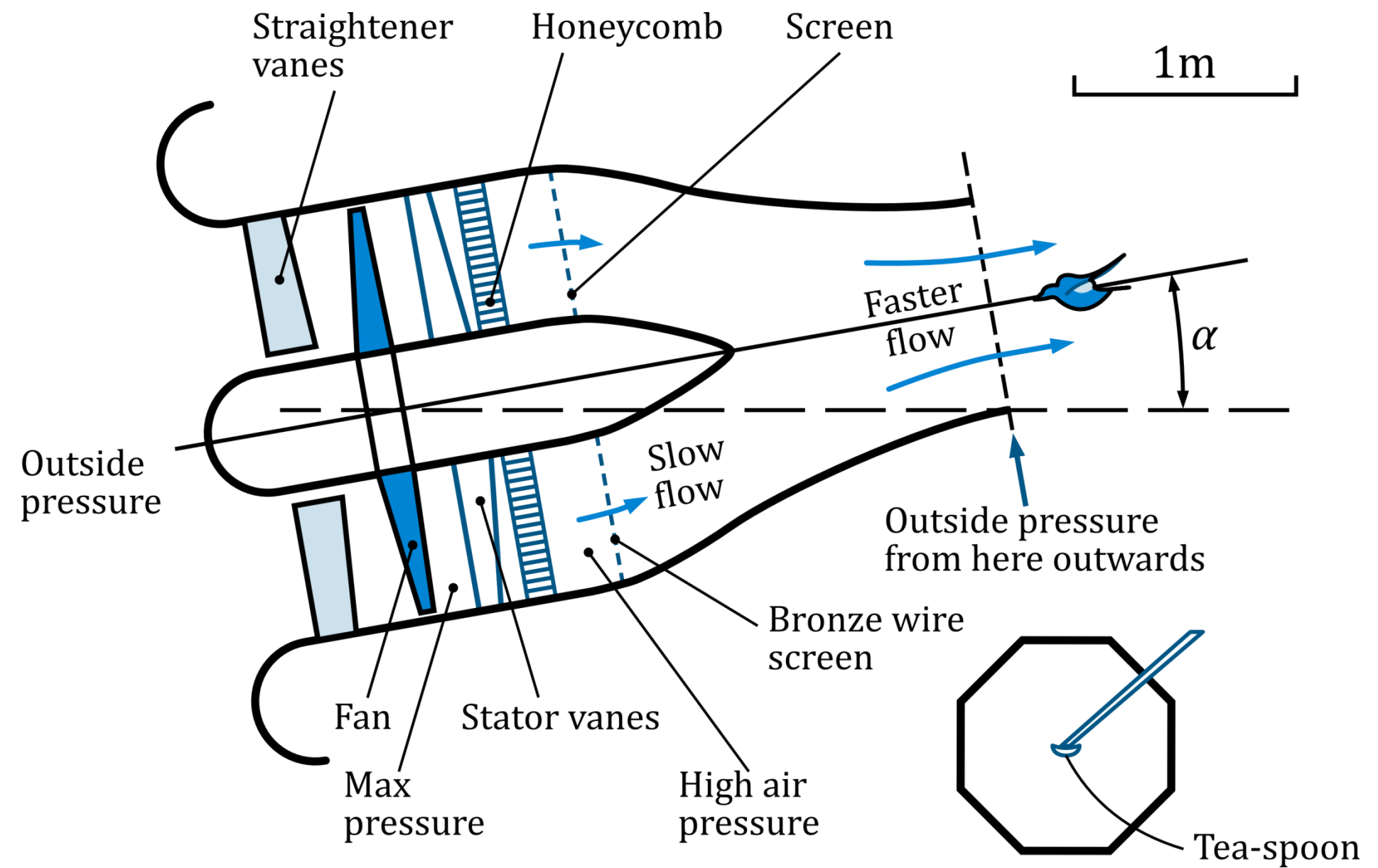


(b) 11.4 m/s

Bird wind tunnel



Outlines traced from overhead photographs of a pigeon gliding steadily at various speeds: (a) 8-6 m/s, span 65 cm; (b) 12.4 m/s, span 57 cm; 22.1 m/s, span 25 cm

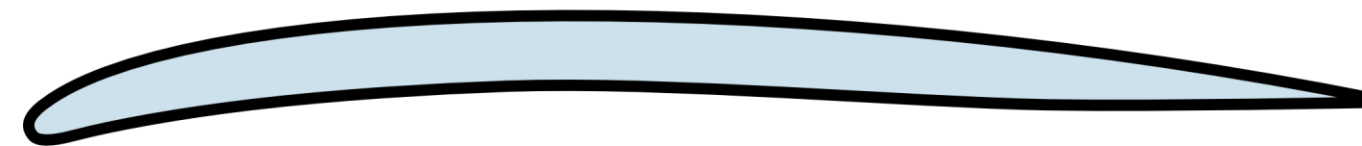


Historical note

World War I



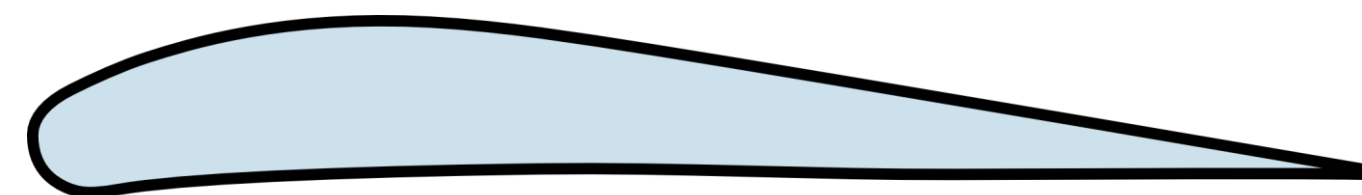
Eiffel 14, French



RAF 14, British



Albatros, German



Gottingen 298, German

Why the early airfoils were so thin?

1917, Gottingen aerodynamic
laboratory of Ludwig Prandtl

$$t/c = 13\%$$

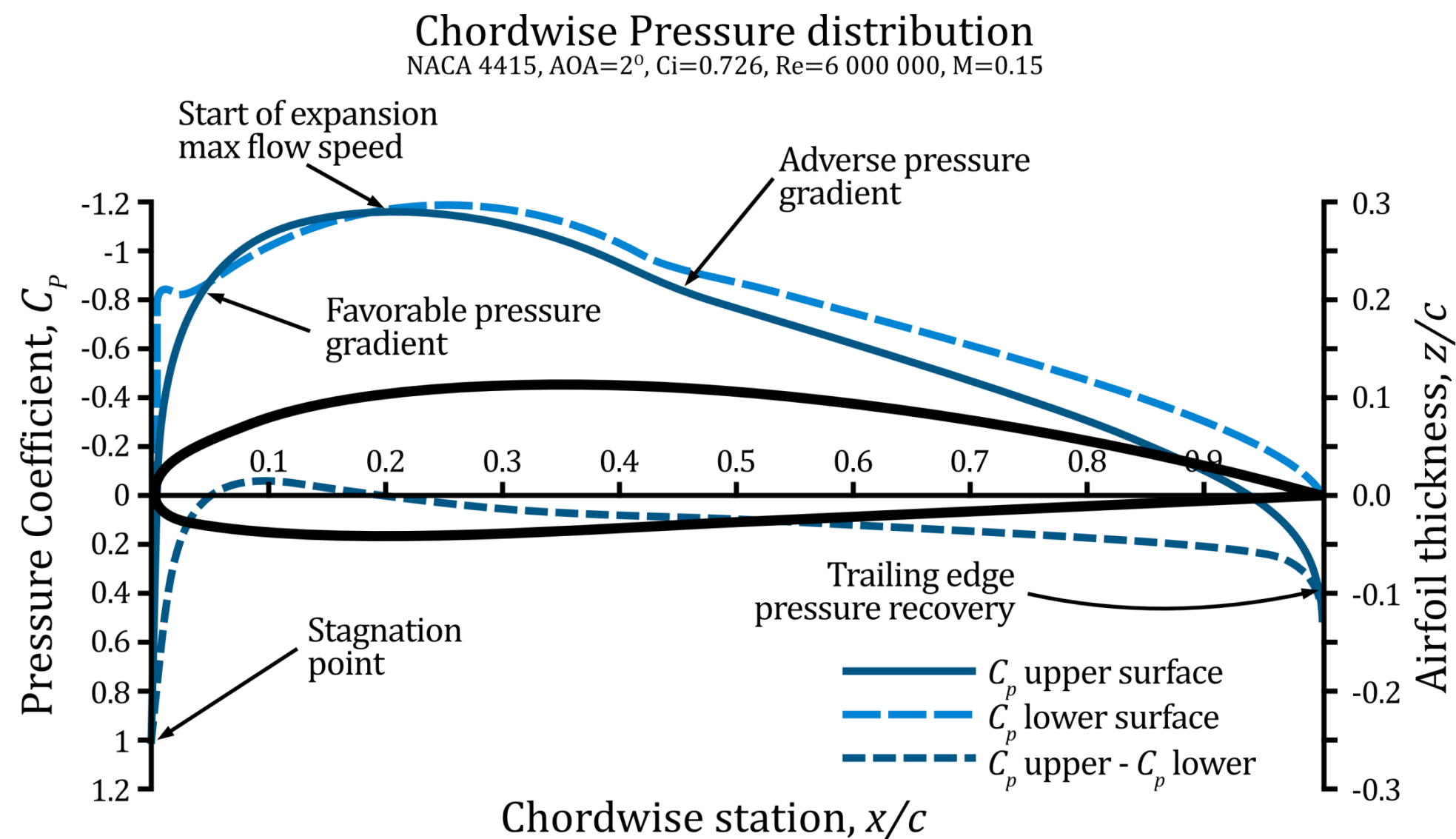
Historical note

Fokker Dr-1

- Internal structures
- Higher $C_{L,max}$



Airfoil chordwise pressure distribution



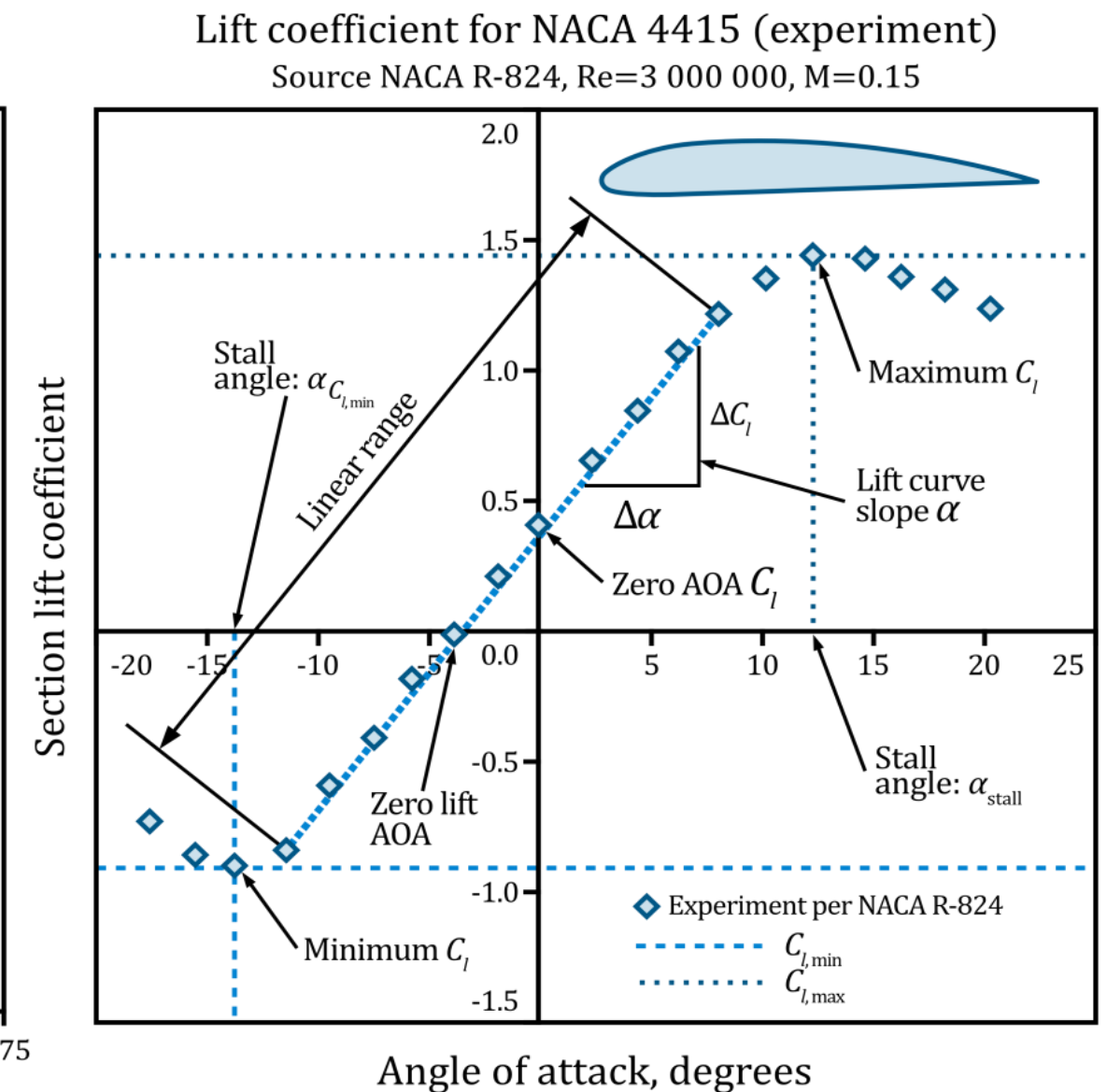
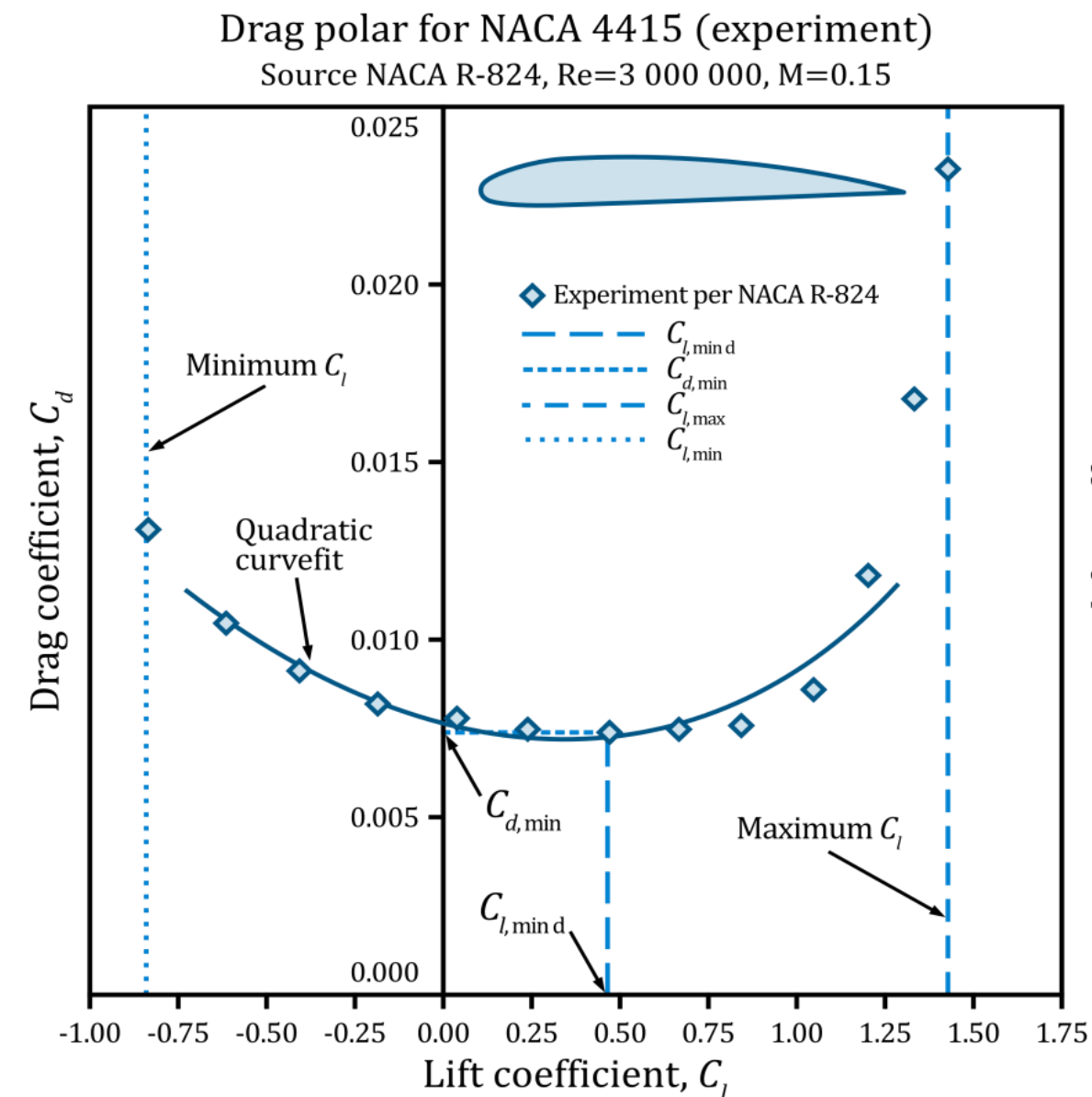
$$C_p \equiv \frac{p - p_\infty}{q_\infty} = 1 - \left(\frac{V}{V_\infty} \right)^2$$

- Determination of structural loads
- The magnitudes of drag, lift, pitching moment,
- Shock formation
- Laminar-to-turbulent boundary layer transition
- Hinge moments

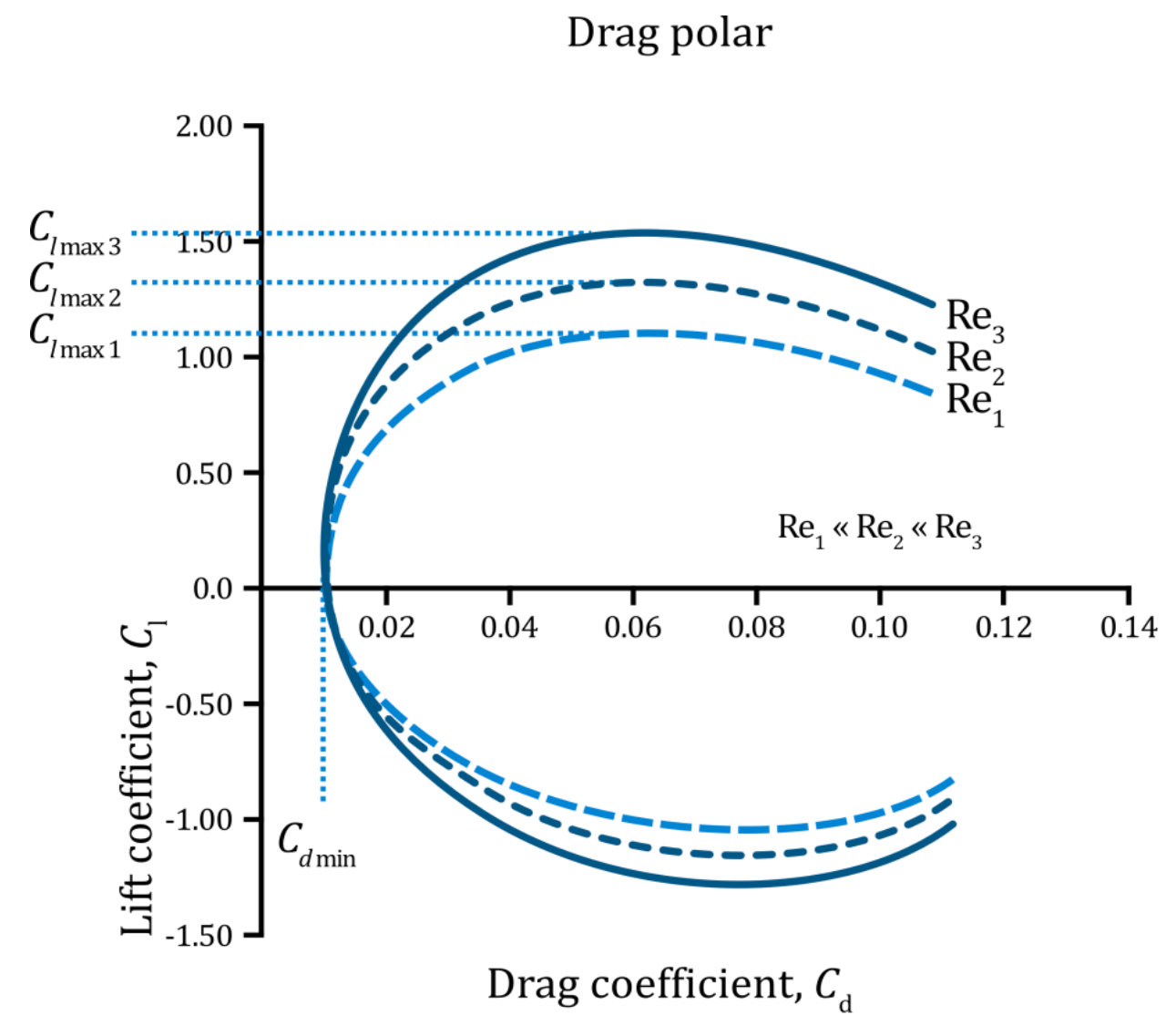
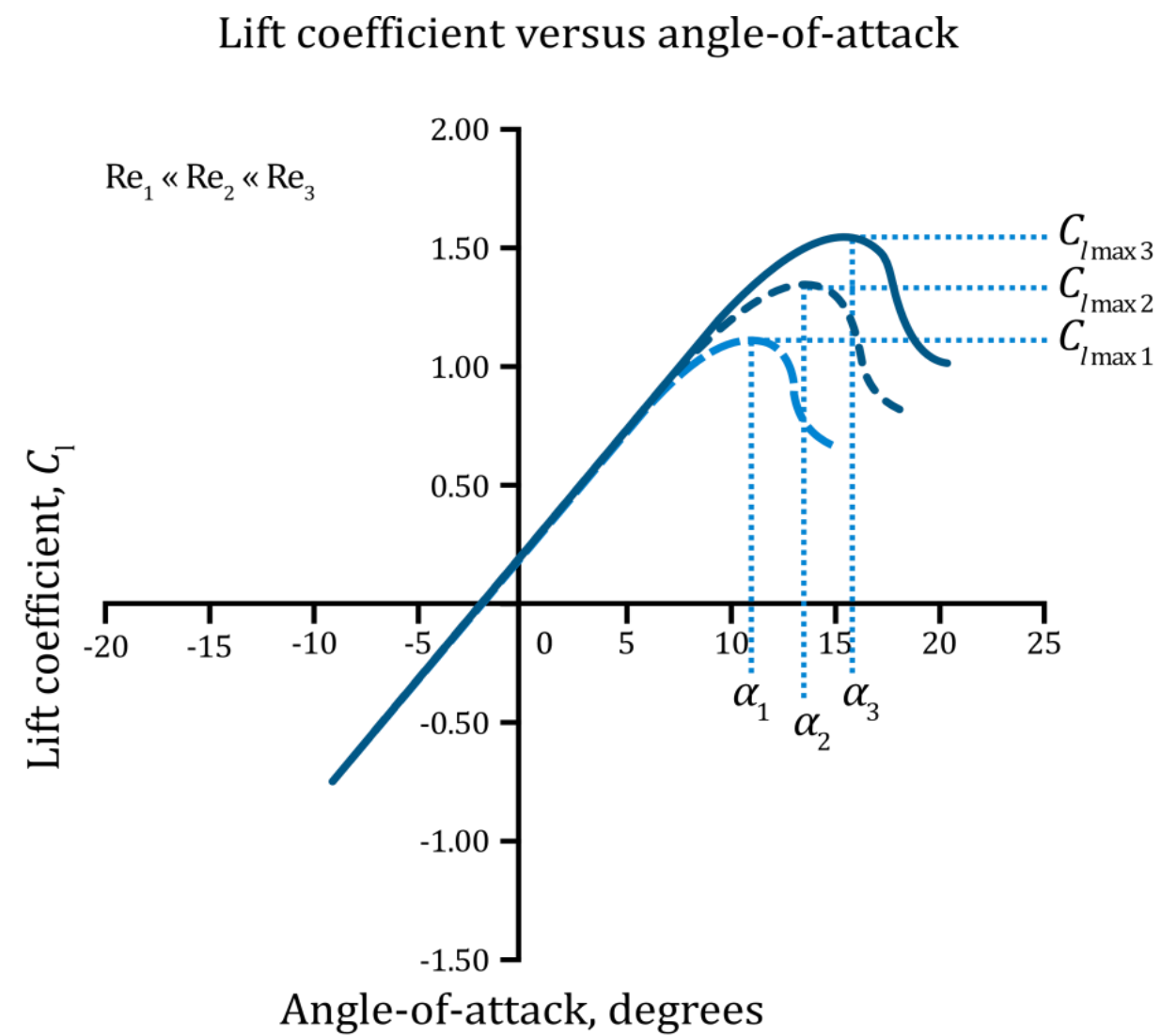
Properties of Typical Airfoils

- Section Lift Coefficient, C_l
- Maximum and Minimum Lift Coefficients, $C_{l,max}$ and $C_{l,min}$
- Lift Curve Slope, a_0
- Angle-of-attack at Zero Lift, $\alpha_{L=0}$
- Linear Range
- Minimum Drag Coefficient, $C_{d,min}$

$$C_l = C_{l,\alpha=0} + a_0 \alpha$$



The Effect of Reynolds Number



The Effect of Reynolds Number

Laminar BL

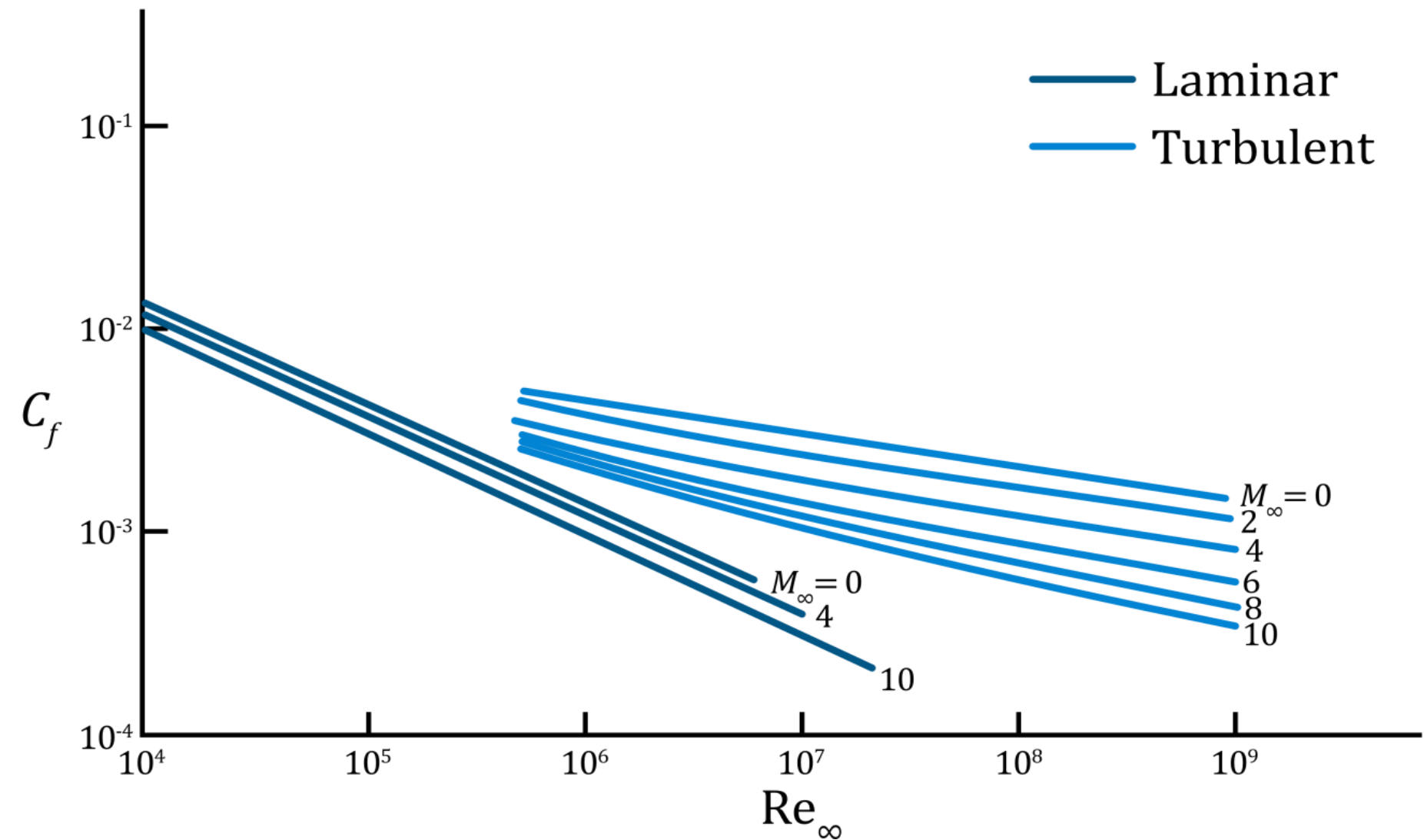
$$C_{f,lam} = \frac{1.328}{\sqrt{Re_c}}$$

$$\delta_{lam} = \frac{5.0x}{\sqrt{Re_x}}$$

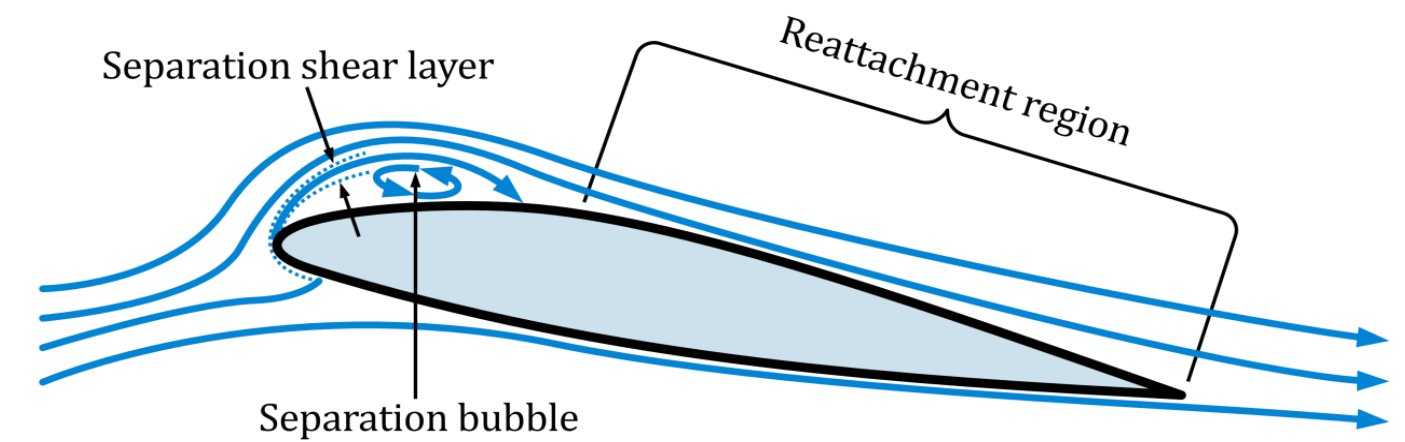
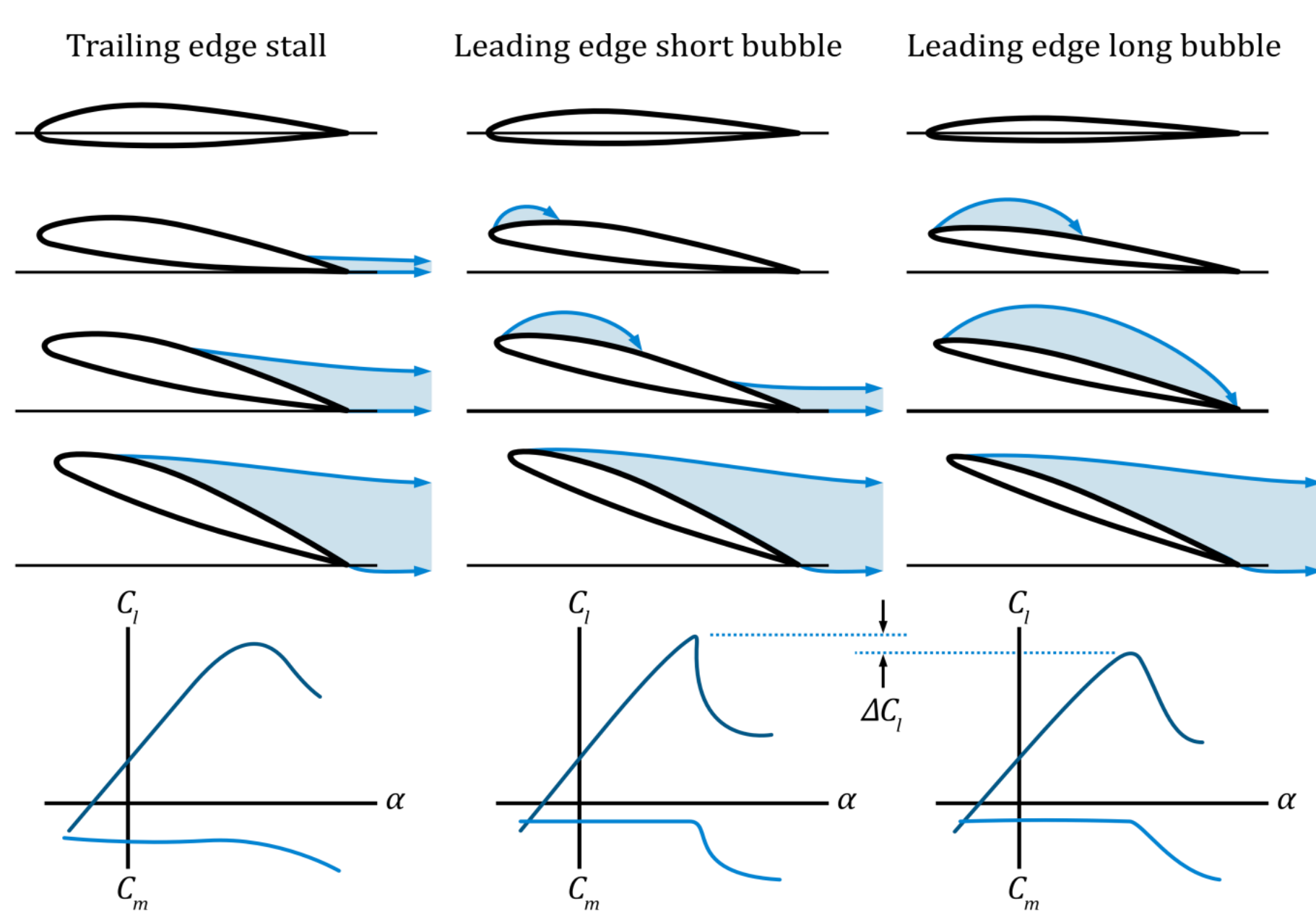
Turbulent BL

$$C_{f,turb} = \frac{0.074}{Re_c^{1/5}}$$

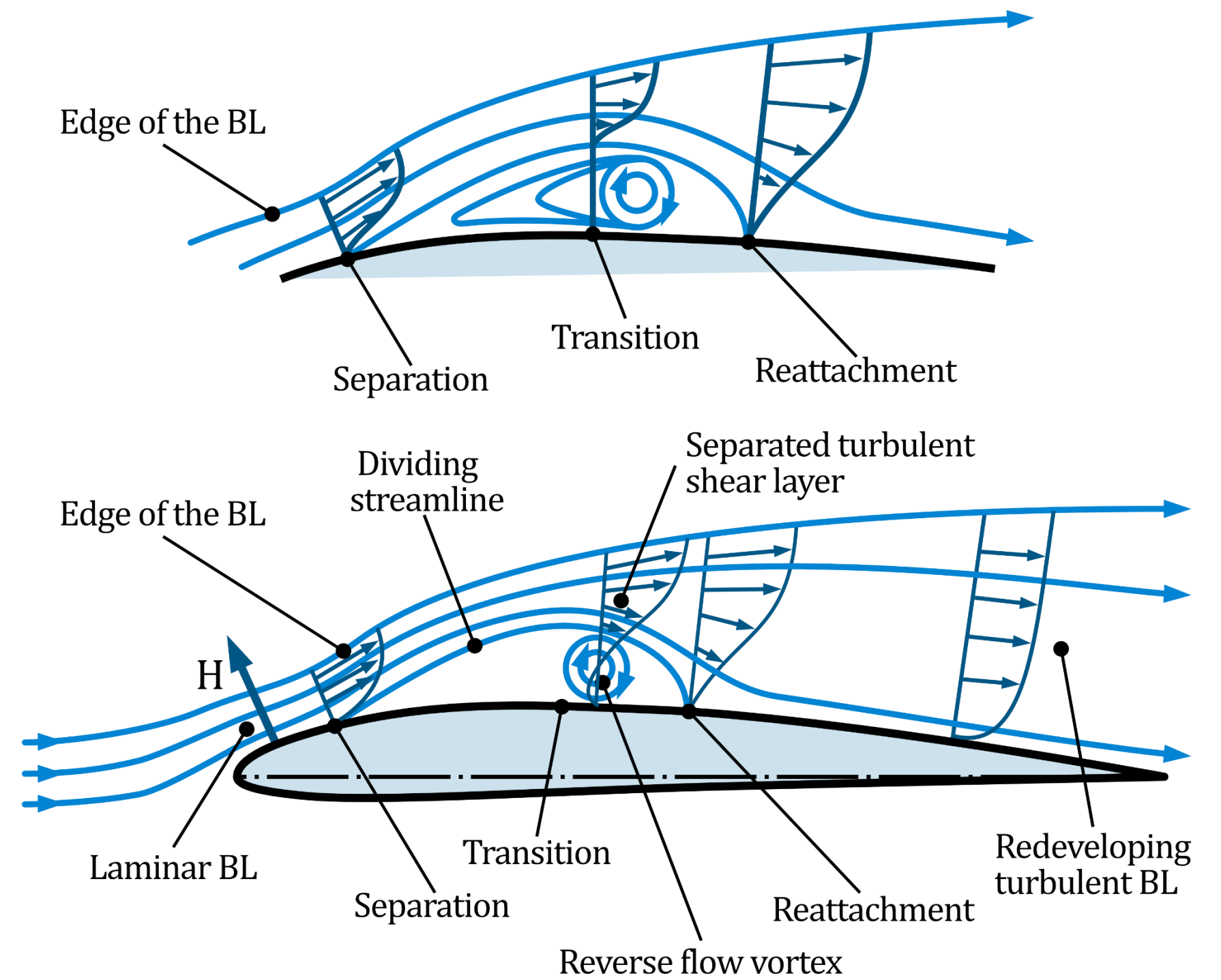
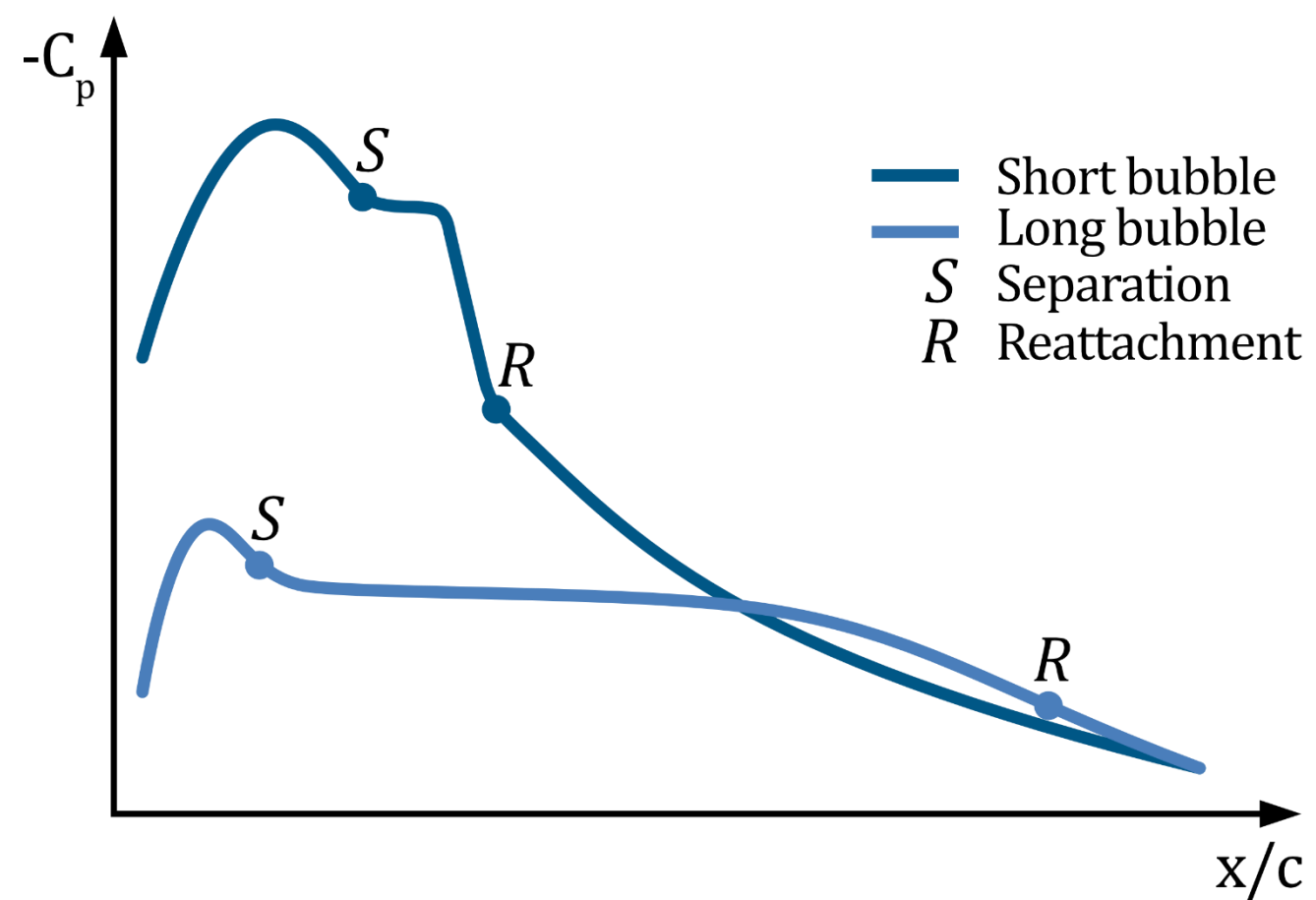
$$\delta_{turb} = \frac{0.37x}{Re_x^{1/5}}$$



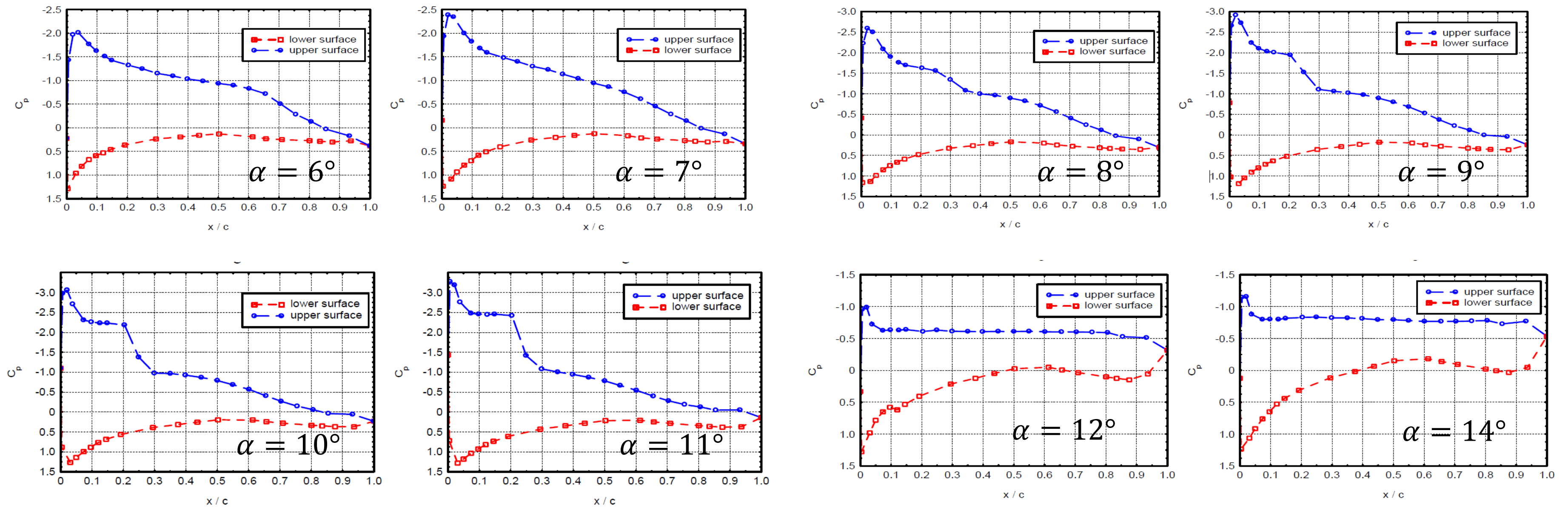
Airfoil Stall Characteristics



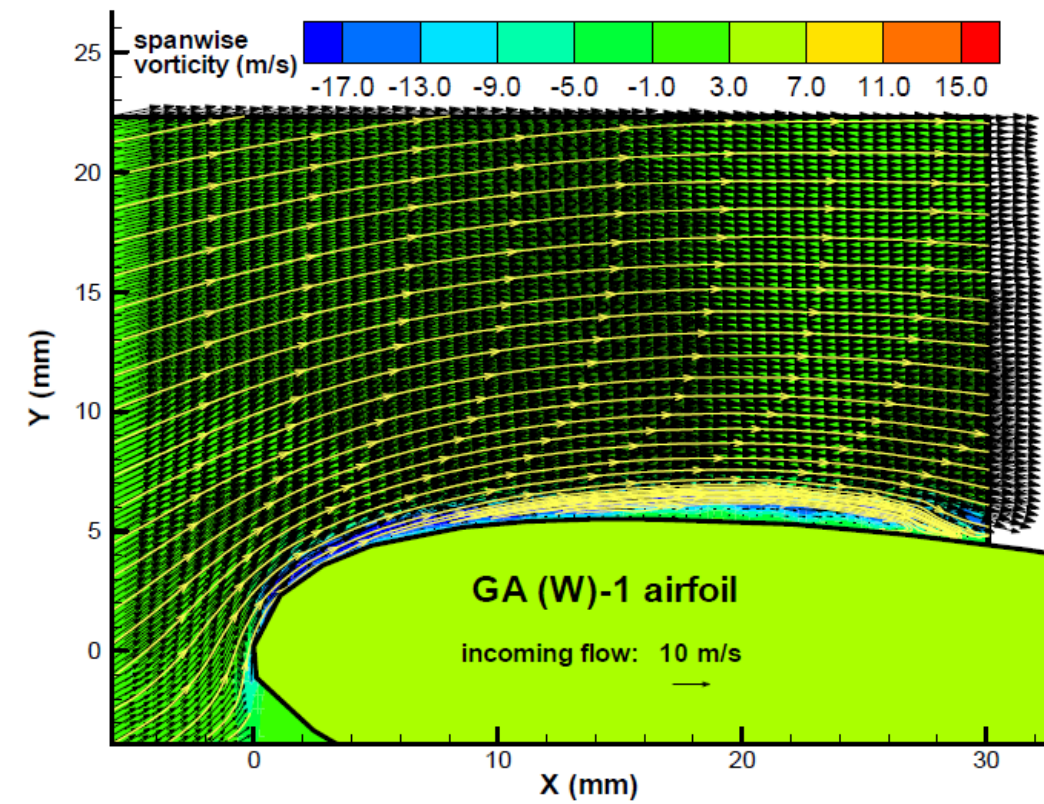
Laminar Bubble



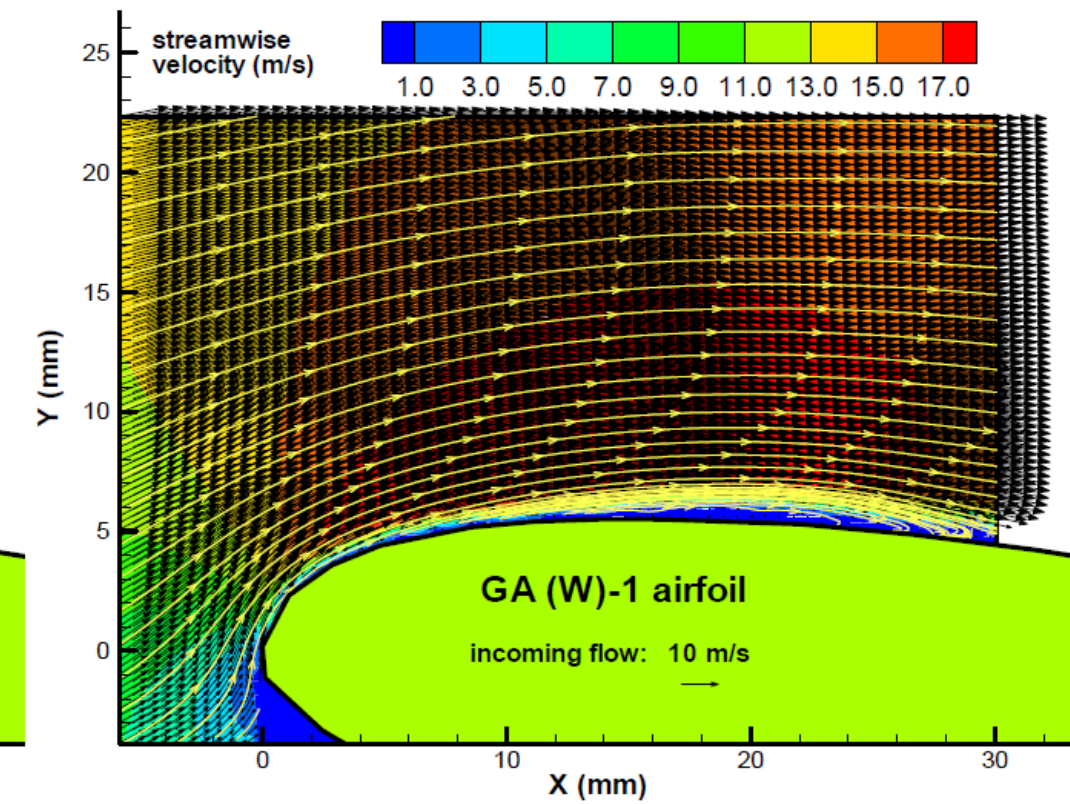
An Experimental Investigation on the Flow Separation on a Low-Reynolds-Number Airfoil: C_p distributions for $Re = 68\,000$



Refined PIV measurements near the nose of the airfoil ($Re = 68\,000$)

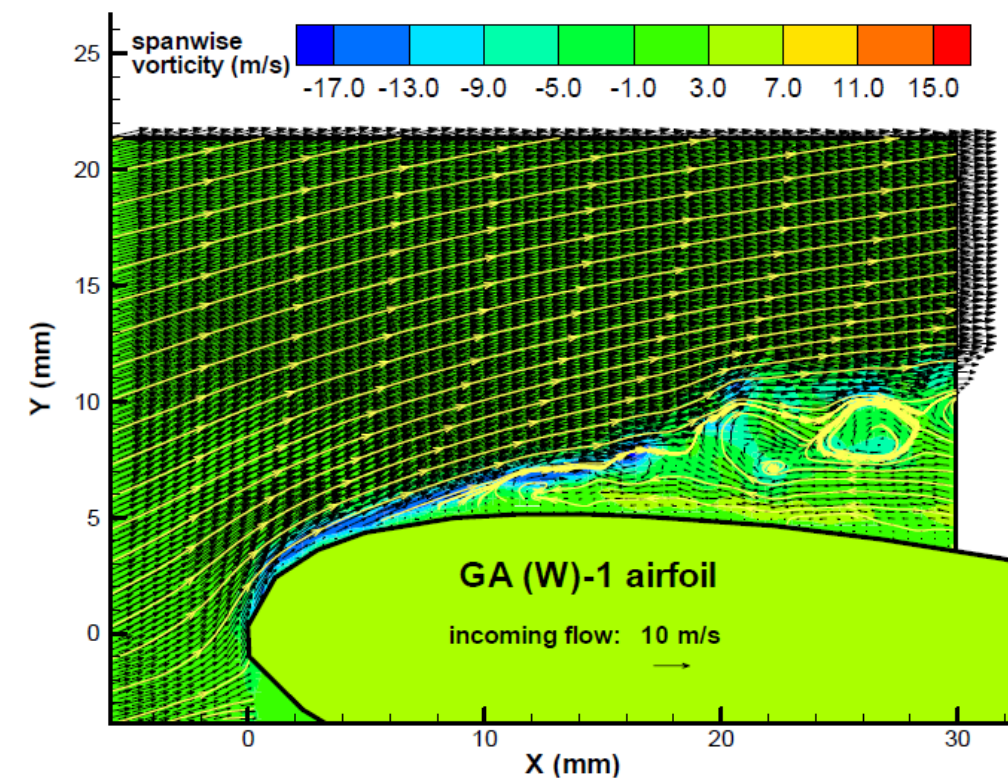


a. Instantaneous measurement result

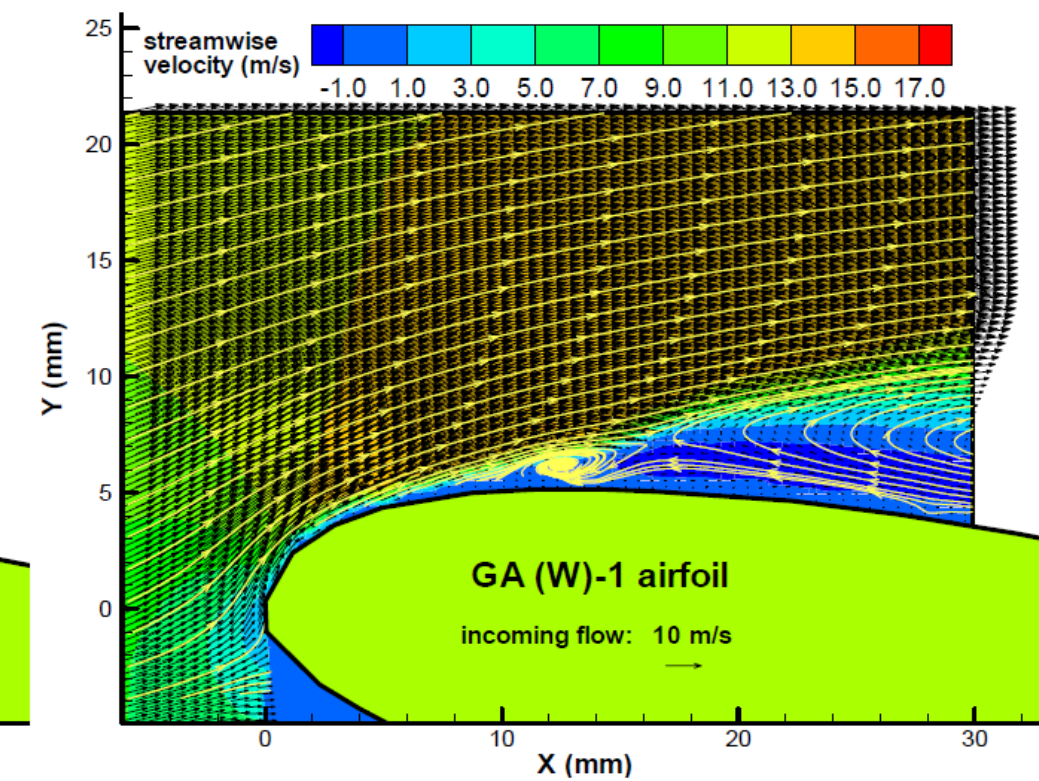


b. Ensemble-averaged measurement result

B. AOA = 10 degrees



a. Instantaneous measurement result



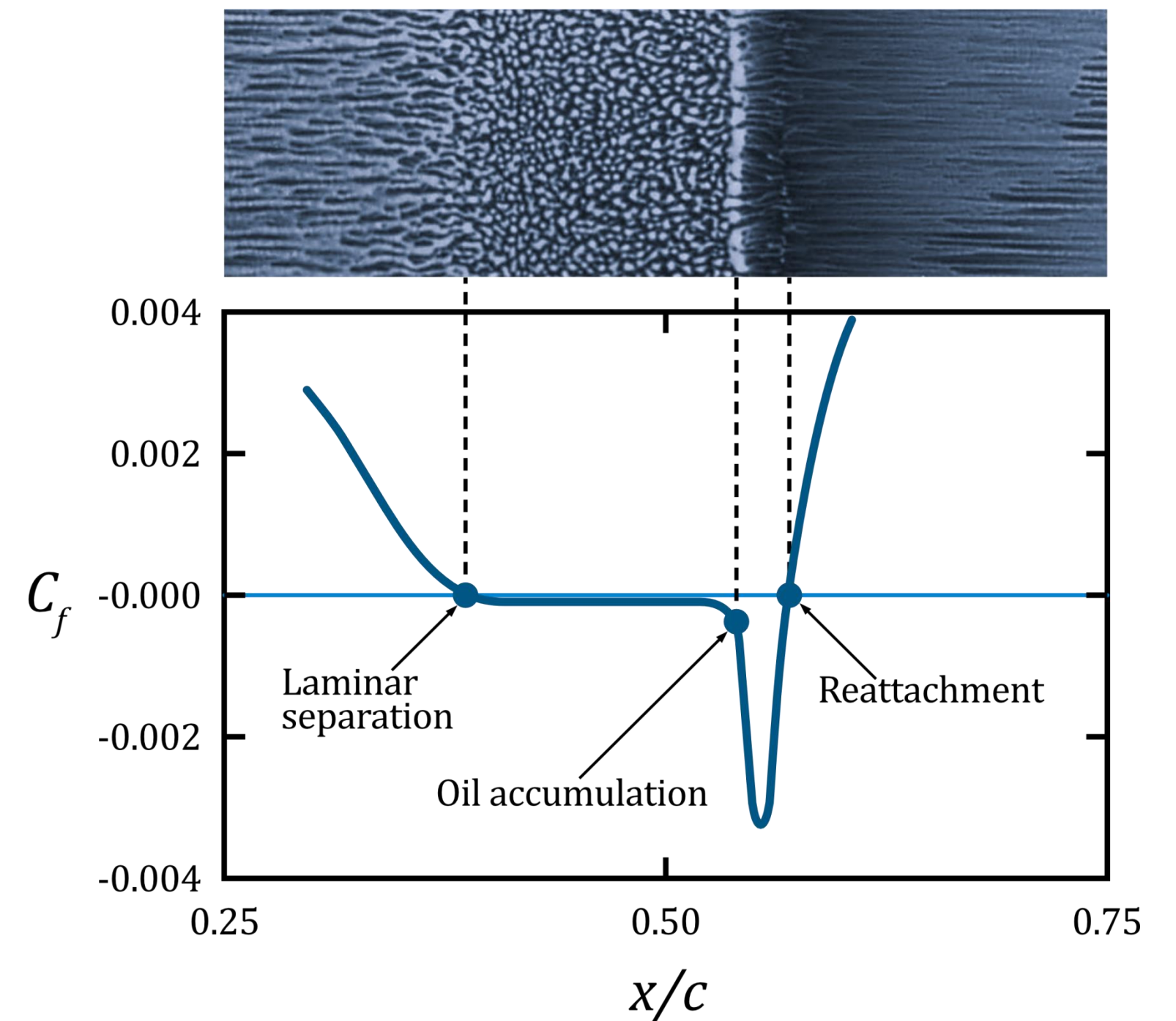
b. Ensemble-averaged measurement result

C. AOA = 12 degrees

Yang, Zifeng, Fred L. Haan, Hui Hu and Hongwei Ma. "An Experimental Investigation on the Flow Separation on a Low-Reynolds-Number Airfoil."

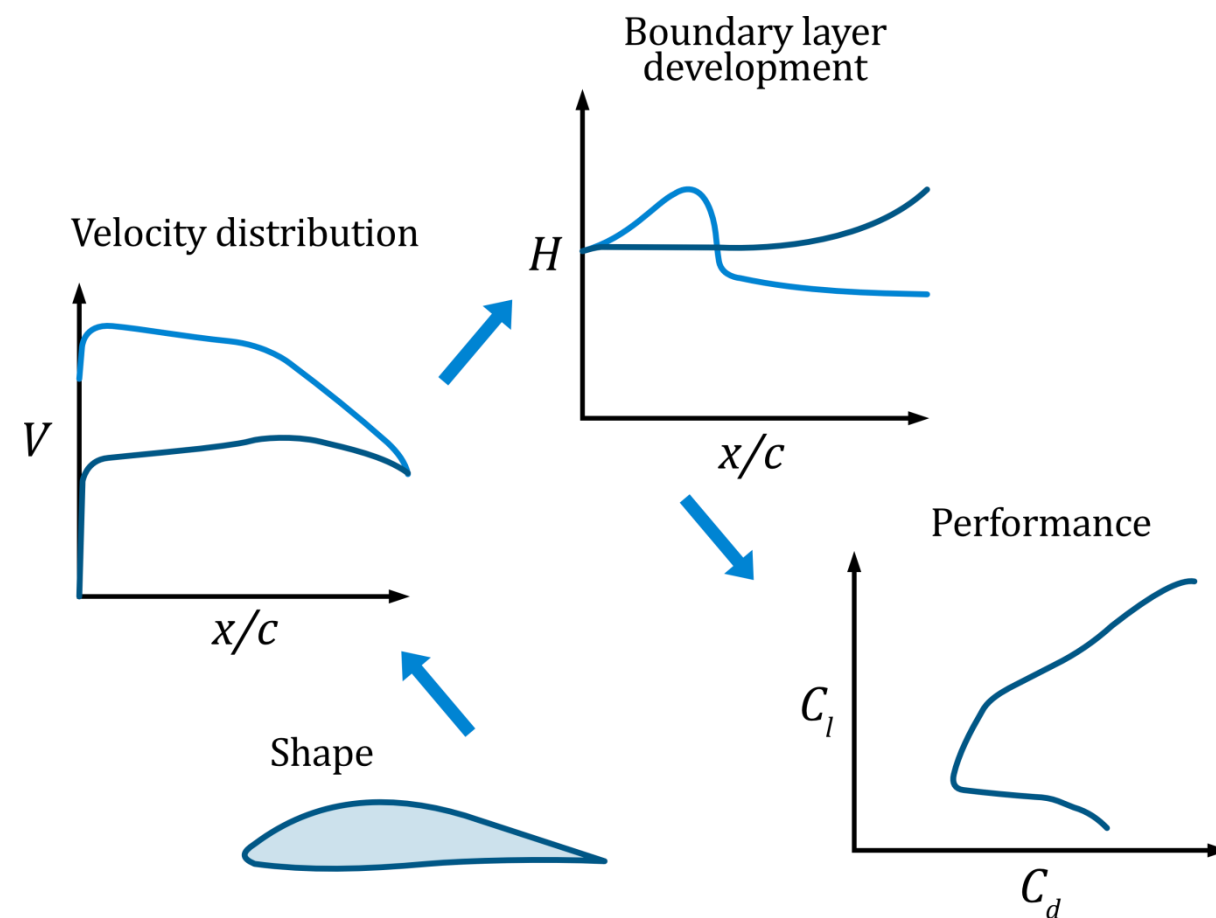
Surface oil flow visualization technique

Conceptual illustration of the relationship between the surface oil flow features and skin friction distribution in the region of a laminar separation bubble plotted against the airfoil chord length

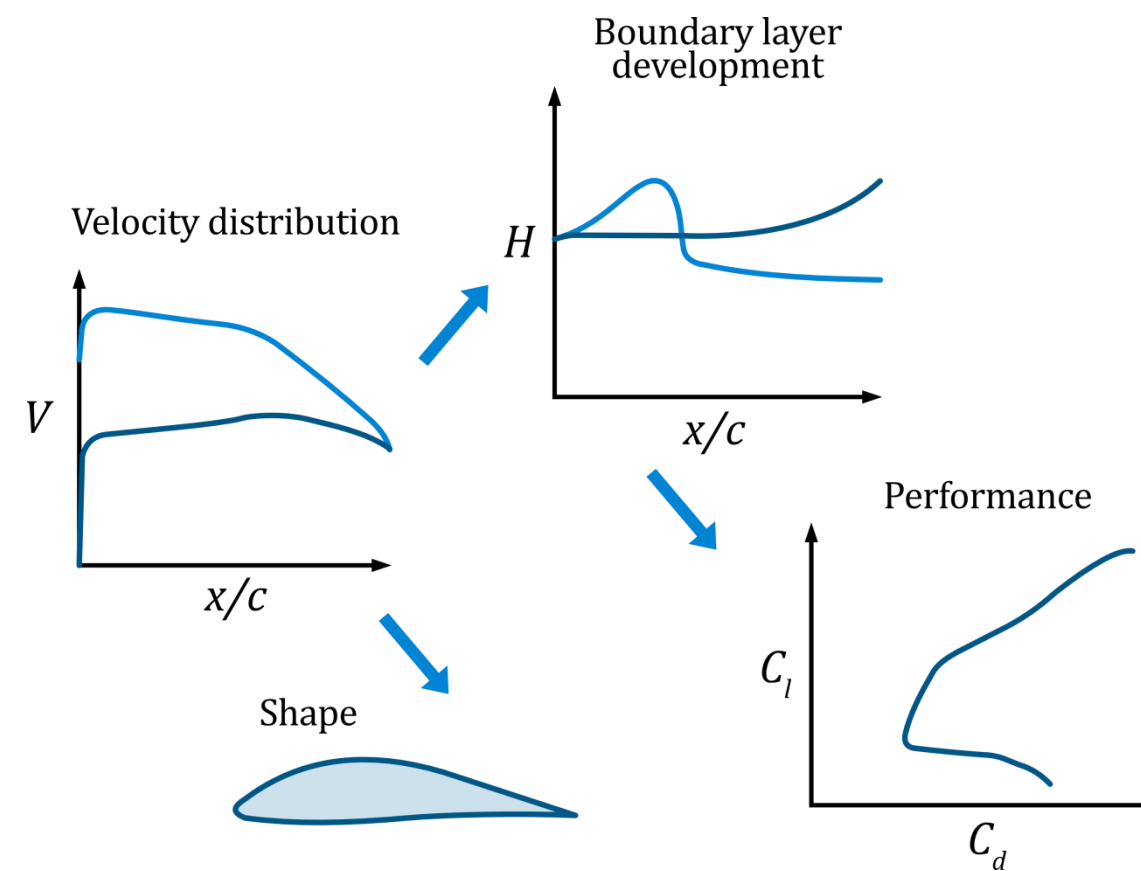


Various Approaches to Airfoil Design

Direct design methods



Inverse method via velocity distributions

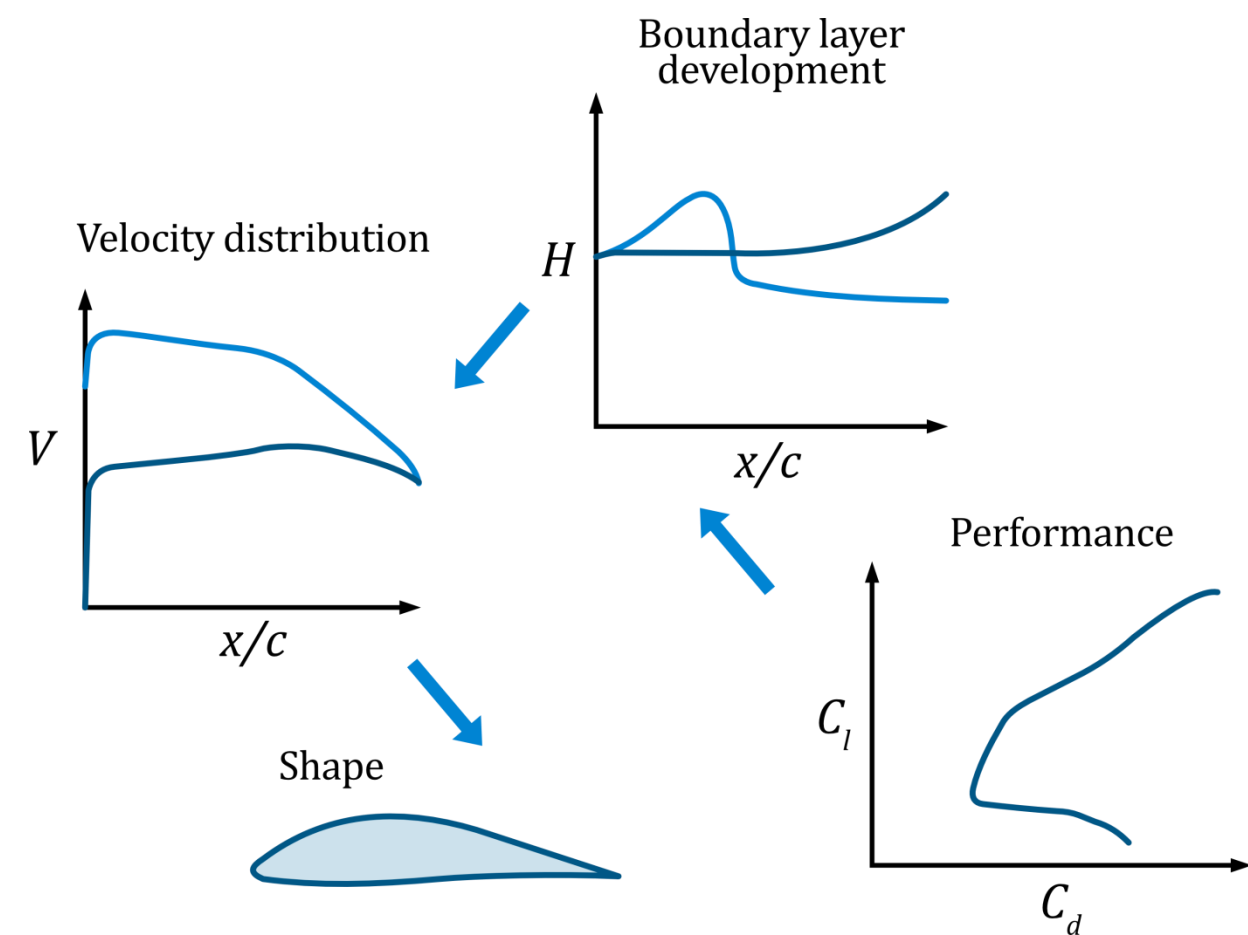


Design variables:

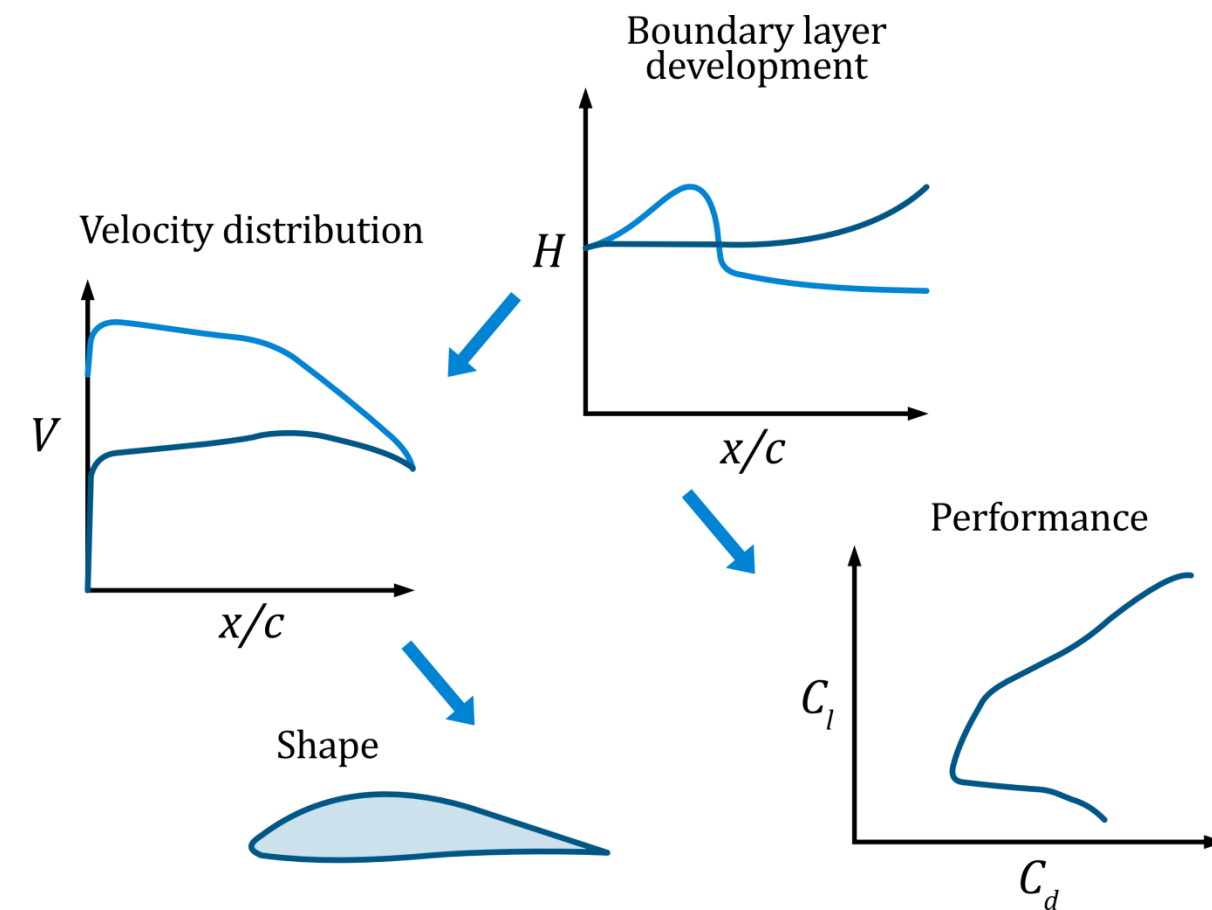
- velocity distribution,
- boundary layer developments,
- airfoil geometry, and
- performance

Various Approaches to Airfoil Design

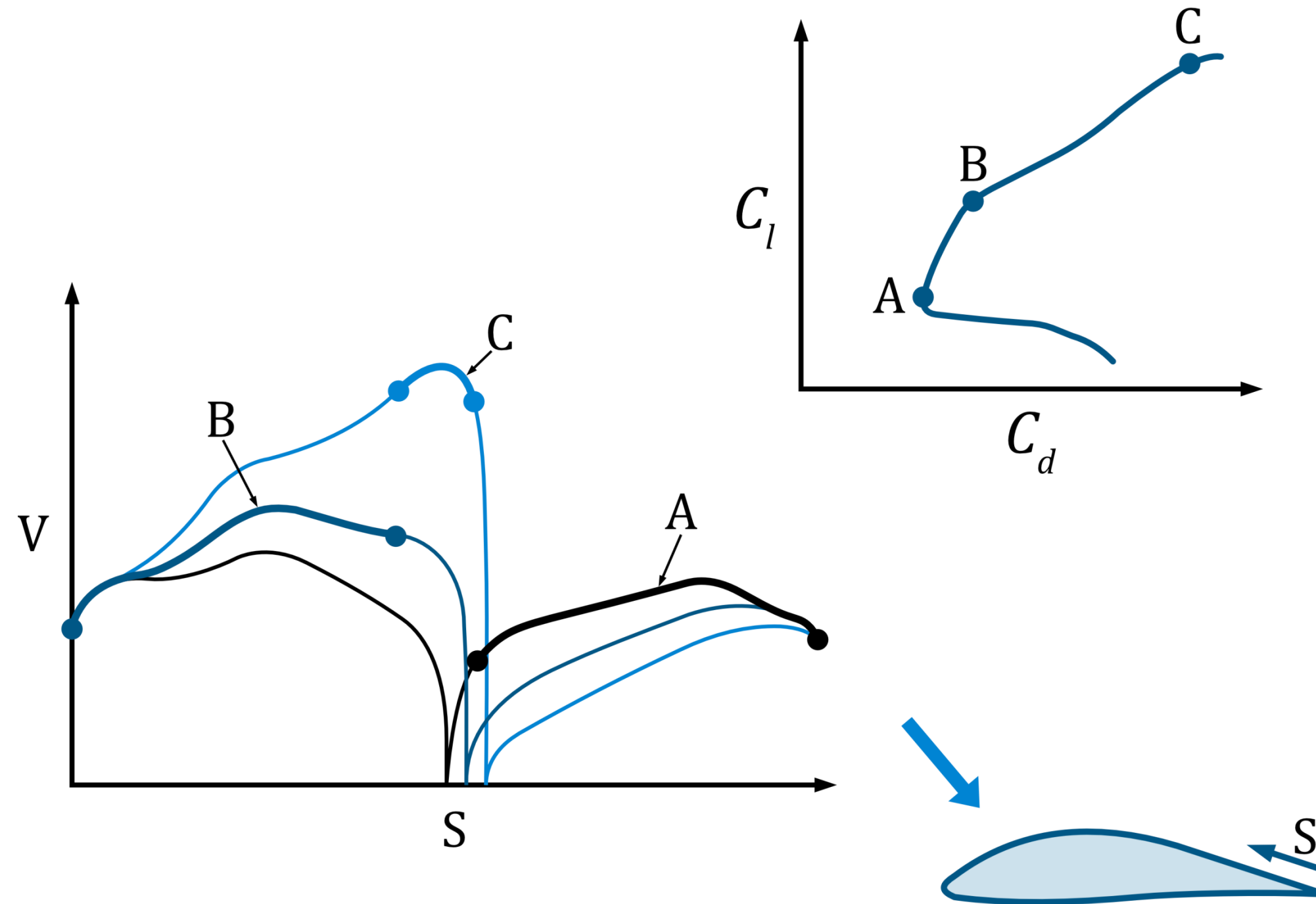
Optimization methods that optimize performance



Inverse viscous design



Multipoint design



Desired Airfoil Characteristics

A drag polar featuring a wide drag bucket is always more desirable than without one

1. Design Lift Coefficient:

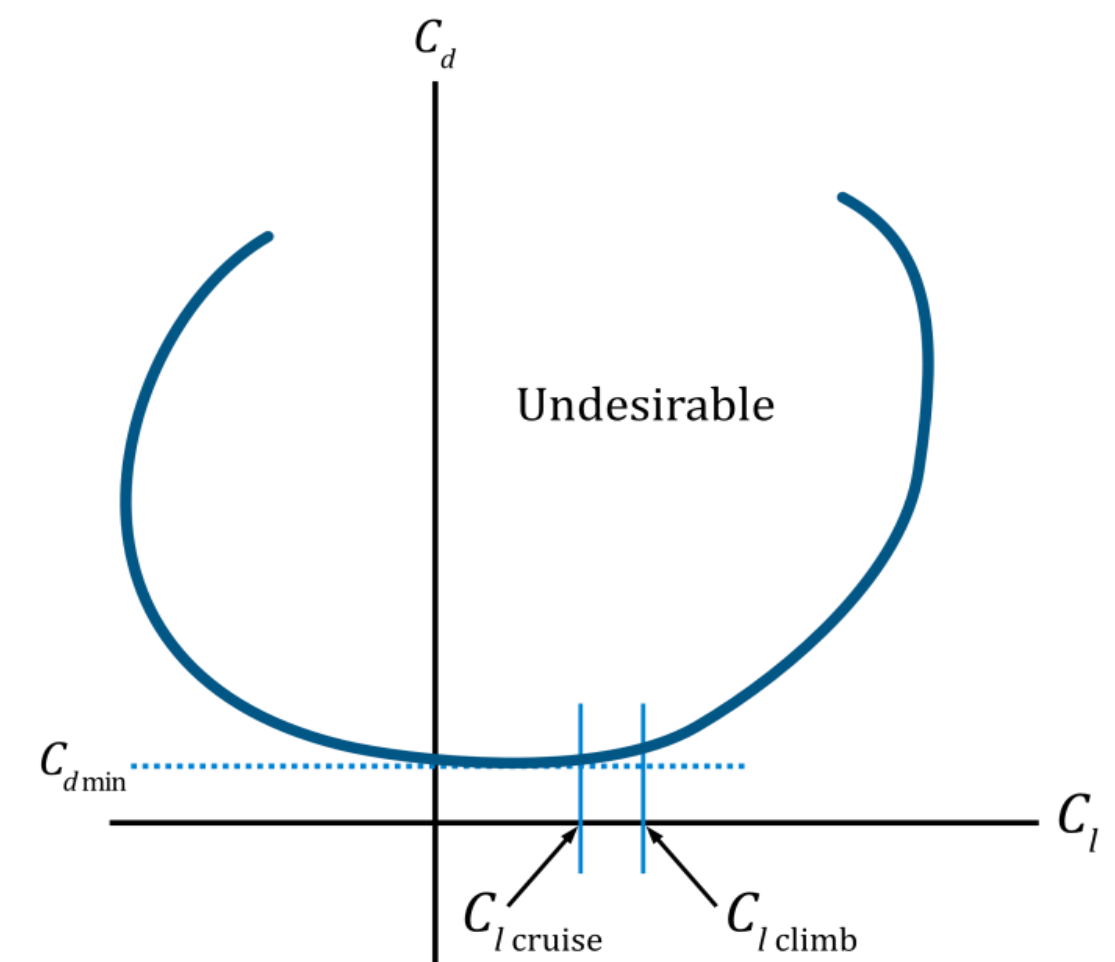
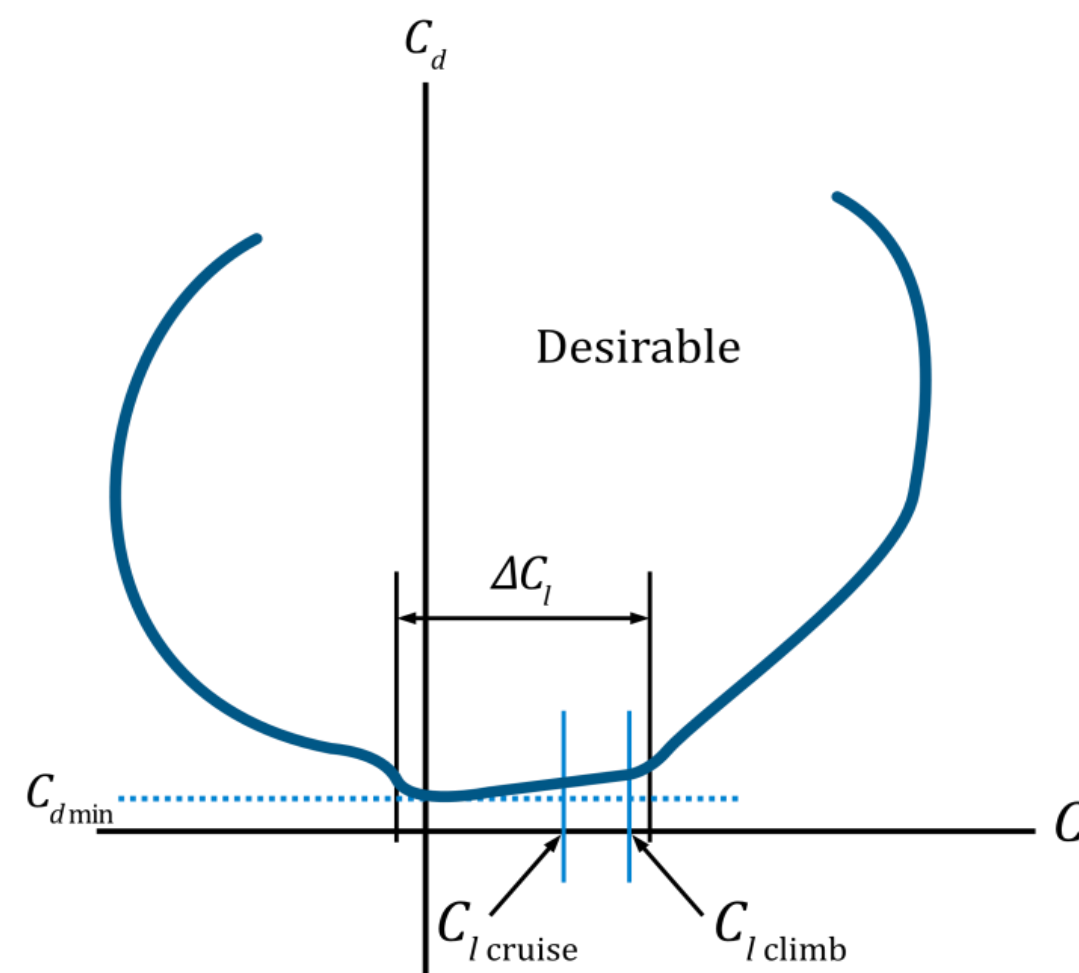
$$W \approx L \approx qSC_L \approx qSC_l, C_l = \frac{1}{q} \left(\frac{W}{S} \right).$$

2. Wide drag bucket

3. $\uparrow C_{l,max}$ with smooth stall

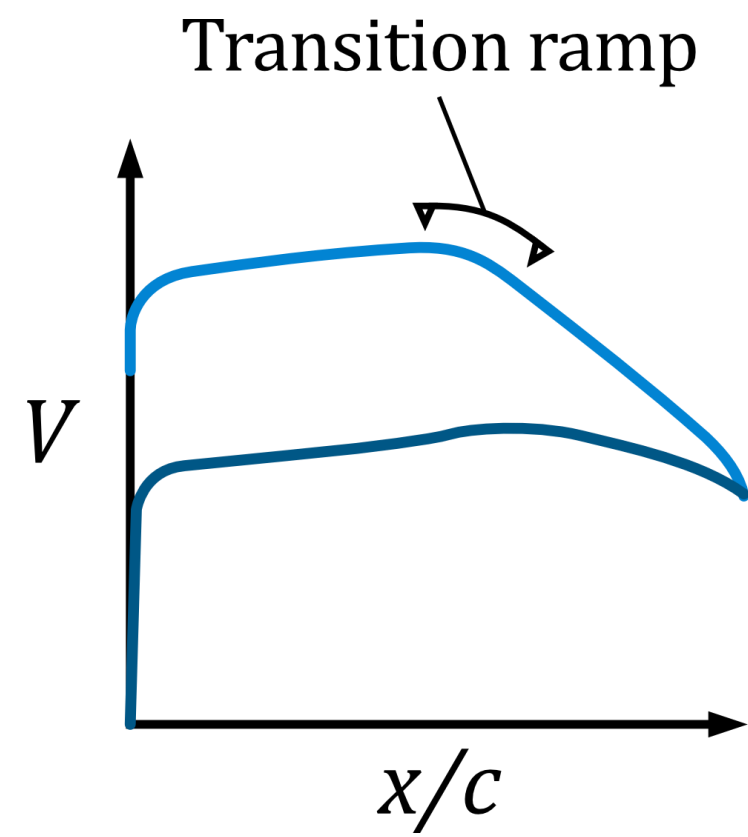
4. $\downarrow C_{m,c/4}$

5. $L/D_{cruise} \rightarrow L/D_{max}$

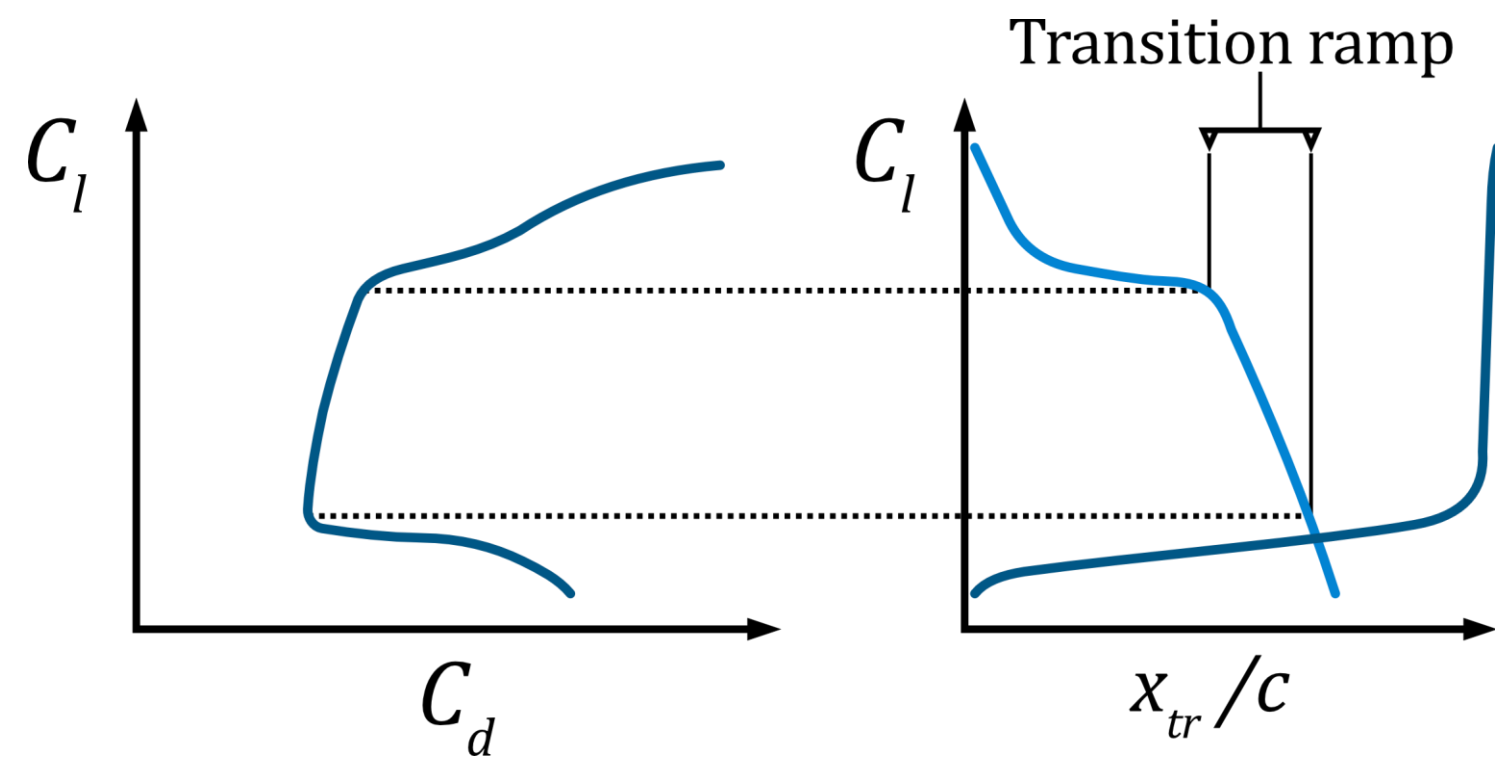


Transition ramp

Conceptual illustration of a transition ramp on the upper surface of an airfoil



Defining the upper surface transition ramp as the chordwise extent over which transition moves while the airfoil operates in the low drag range



Relations between airfoil geometry and performance: summary

Maximum camber location $\bar{X}_{f,max}$:

high $C_{l,max}$ when $\bar{X}_{f,max} = 0,2 \dots 0,3$

high L/D_{max} when $\bar{X}_{f,max} = 0,2 \dots 0,4$

low $C_{d,min}$ when $\bar{X}_{f,max} = 0,4$

Leading-edge radius r :

$r \uparrow \rightarrow$ more smooth stall at α_{cr}

Trailing edge thickness t_{tr} : $t_{tr} \uparrow$

$\rightarrow C_{d,min} \uparrow$

$L/D_{max} \downarrow$

Maximum thickness location $\bar{X}_{t,max}$: $\bar{X}_{t,max} \uparrow$

$\rightarrow C_{d,min} \downarrow$

$C_{l,max} \downarrow$

$C_{d,min} \uparrow$ at high α

Thickness ratio t/c : $t/c \uparrow$

$\rightarrow \uparrow$ structural depth and inner volume of the wing

\downarrow the weight of the wing

\uparrow wing structural stiffness

$\uparrow C_{d,min}$

$\uparrow C_{l,max}$ (for thickness ratios of 0,13... 0,16)

$\downarrow L/D_{max}$

Camber ratio f/c : $f/c \uparrow$

$\rightarrow C_{l,max} \uparrow$

$C_{d,min} \uparrow$

$L/D_{max} \downarrow$

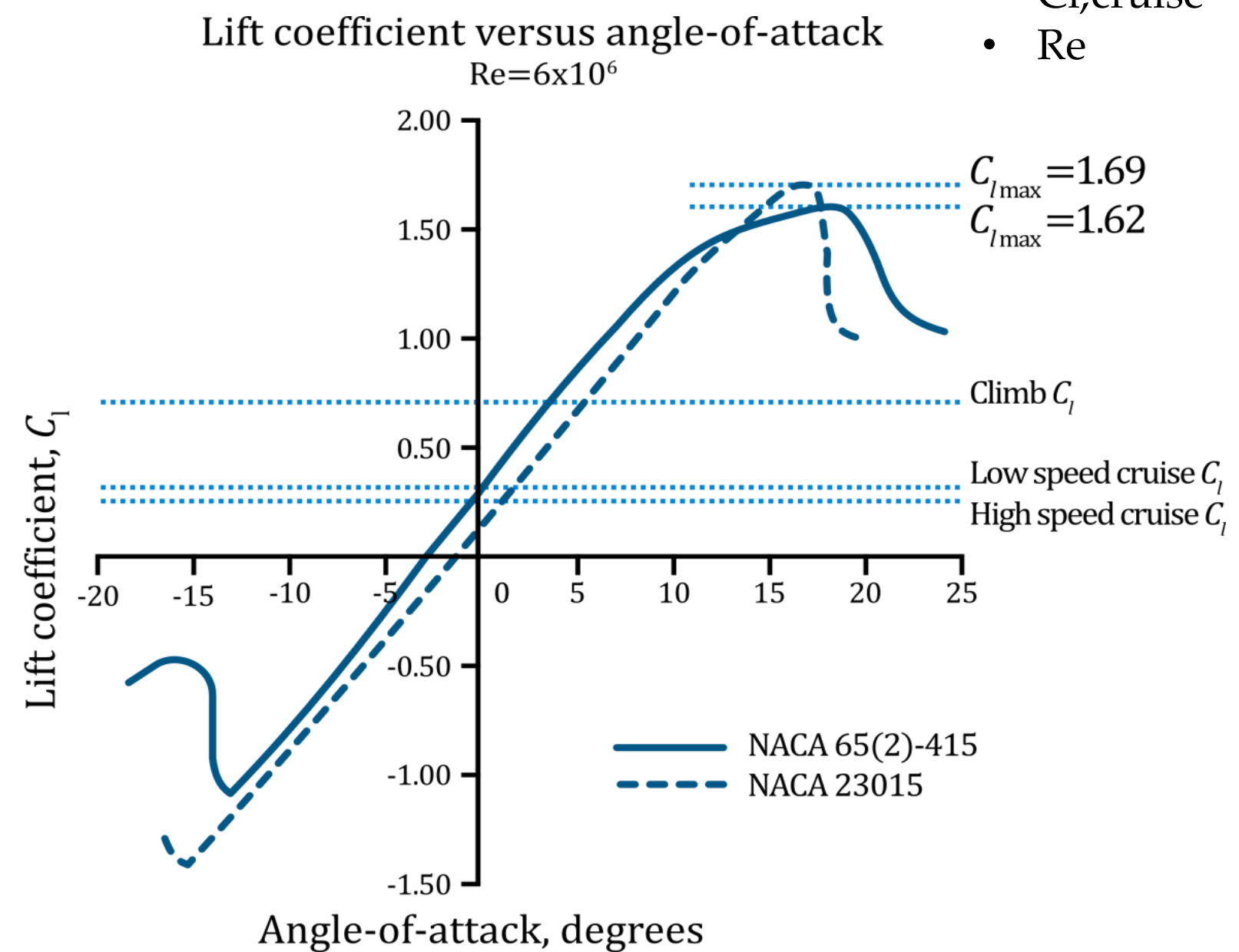
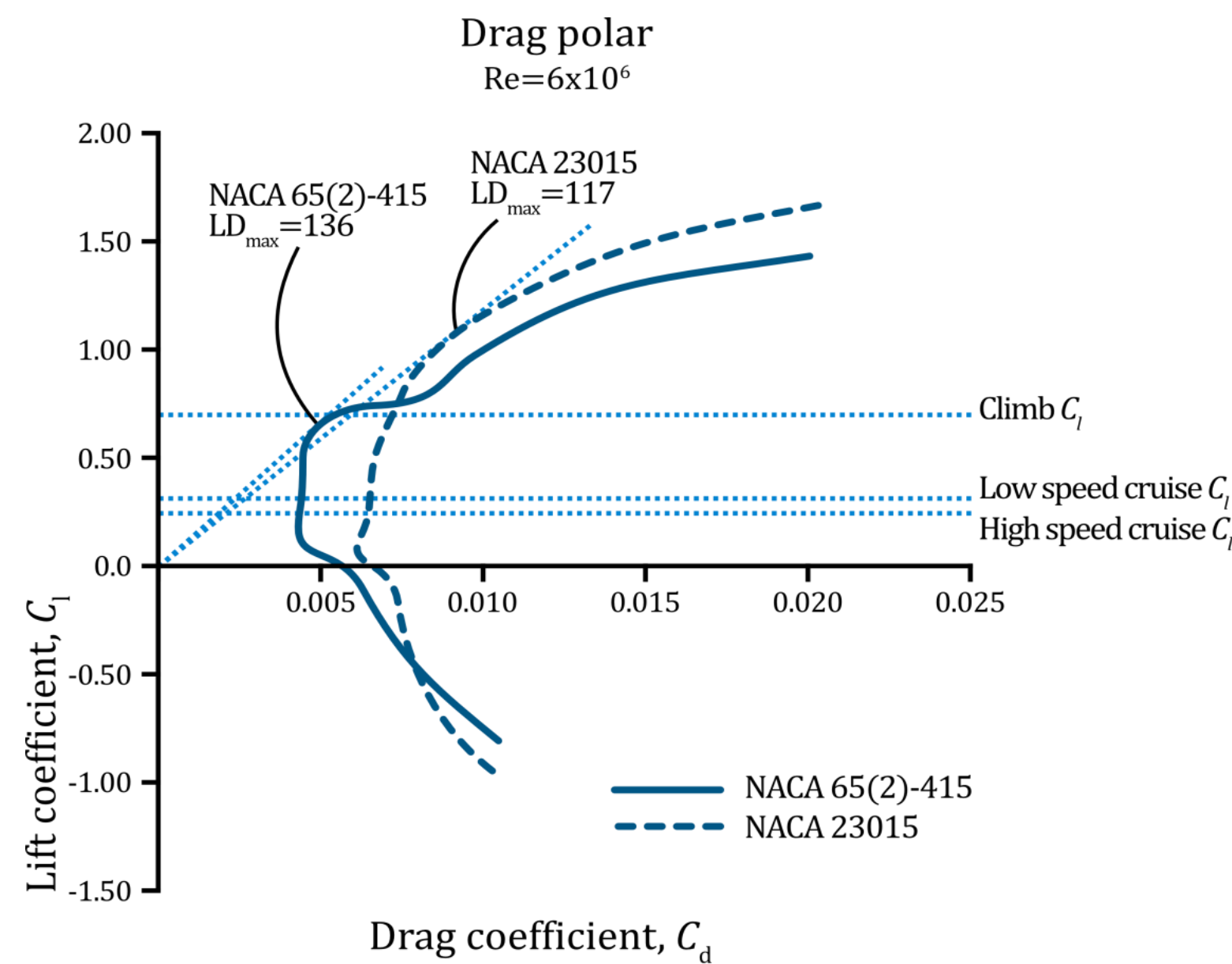
$\alpha_0 \uparrow$

$C_{m0} \uparrow$

\uparrow center of pressure displacement

Desired Airfoil Characteristics

- $C_{l,max}$
- Stall, including stalling speed
- L/D at $C_{l,climb}$
- $C_{l,cruise}$
- Re



Some trends in the design of airfoils for low Reynolds numbers

- The desired pressure distribution which should sustain laminar flow is where the pressure decreases with distance from the leading edge over the forward portion of the airfoil.
- At Reynolds number below 1 million, a transitional separation bubble contributes significantly to the form drag.
- The optimum transition location is usually close to the laminar separation point, before the separated shear layer moves too far from the airfoil surface.
- By maximizing $C_{l,max}/C_{d,min}$, the wing parasite drag is minimized.
- The maximum lift coefficient is not dramatically influenced by leading-edge roughness if turbulent flow is predominant on the upper surface at $C_{l,max}$.
- The widest possible low-drag range is achieved when the laminar boundary layer is held on the verge of laminar separation and then on the verge of boundary-layer transition.
- It is expected to be possible to eliminate the local flow separation only in a very narrow range of angles of attack.

Machine Learning in Aerodynamic Shape Optimization

- Aerodynamic shape optimization significantly **reduces the aircraft development's cycle time** and improves the design's performance.
- **The high computational cost of aerodynamic analysis and the high dimensionality of the geometric design space** are two compounding challenges in ASO
- CFD-based optimization has mostly been deterministic, ignoring aleatory uncertainties in operating conditions or geometry changes due to wear and tear and manufacturing inaccuracies.
- There is still a lack of techniques to utilize different aerodynamic data and models together effectively.
- There are discontinuous ASO problems that are difficult for the current gradient-based frameworks to handle.
- **ML models**, once trained, usually work **without the need to solve for the physics governing equations**, so they are computationally efficient.
- Instead of purely data-fitting, another ML approach is to **train neural networks to respect given physics laws**, which is known as physics-informed neural networks (PINN)

Streamline Curvature and Airfoil Lift Generation

\mathbf{r} is the direction normal to the streamwise direction (pointing along the radius of curvature)

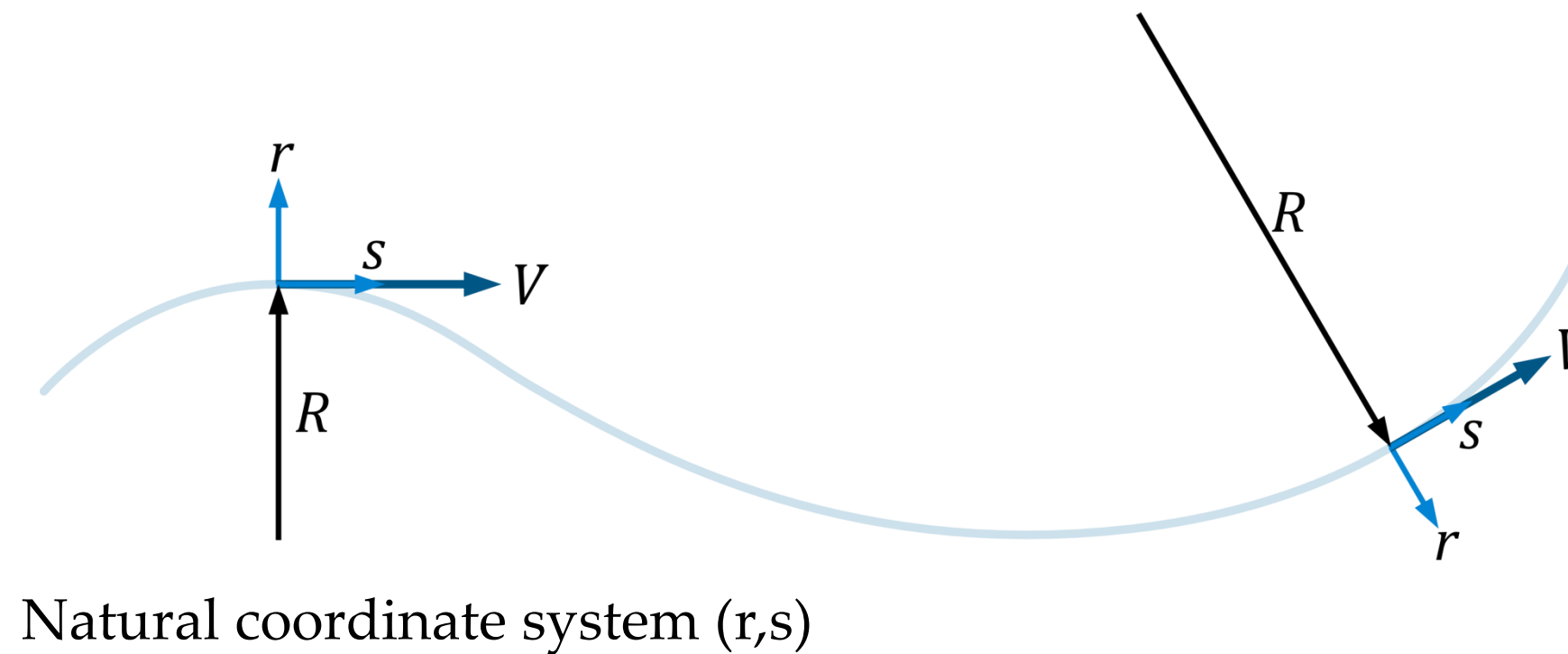
\mathbf{s} is in the streamwise direction (tangent to the velocity vector, V)

R is the magnitude of the radius of curvature

The pressure increases in the radial direction

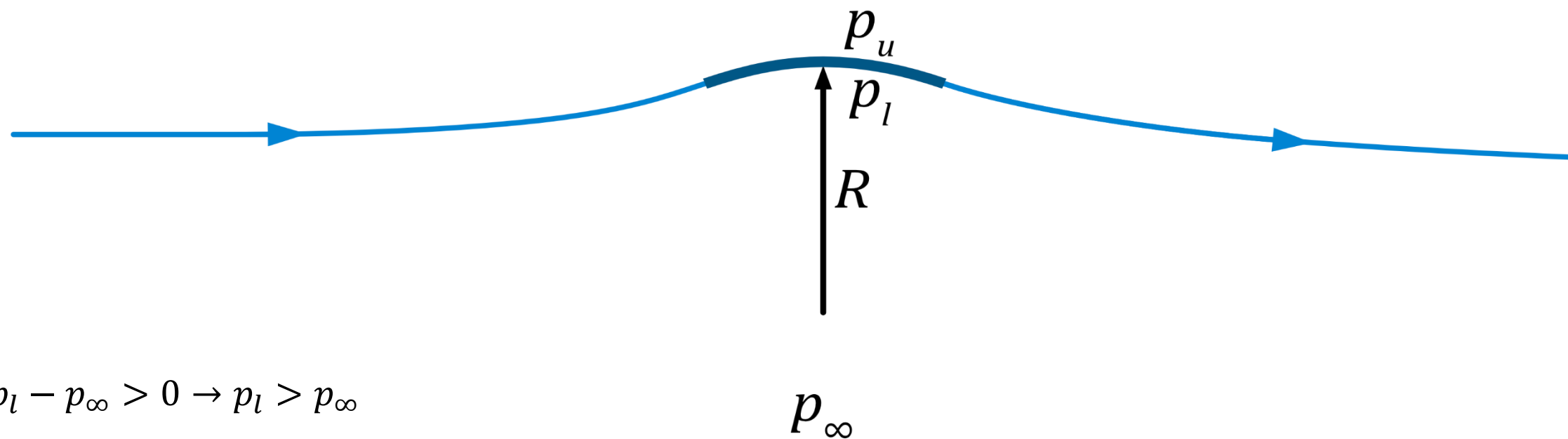
Assumptions: steady, inviscid flow

$$\frac{\partial p}{\partial r} = \rho \frac{V^2}{R}$$



Streamline Curvature and Airfoil Lift Generation

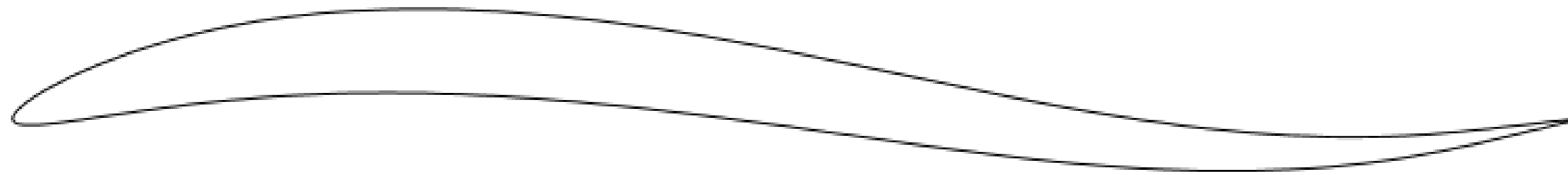
$$\frac{\partial p}{\partial r} = \rho \frac{V^2}{R} > 0 \rightarrow p_\infty - p_u > 0 \rightarrow p_u < p_\infty$$



$$\frac{\partial p}{\partial r} = \rho \frac{V^2}{R} > 0 \rightarrow p_l - p_\infty > 0 \rightarrow p_l > p_\infty$$

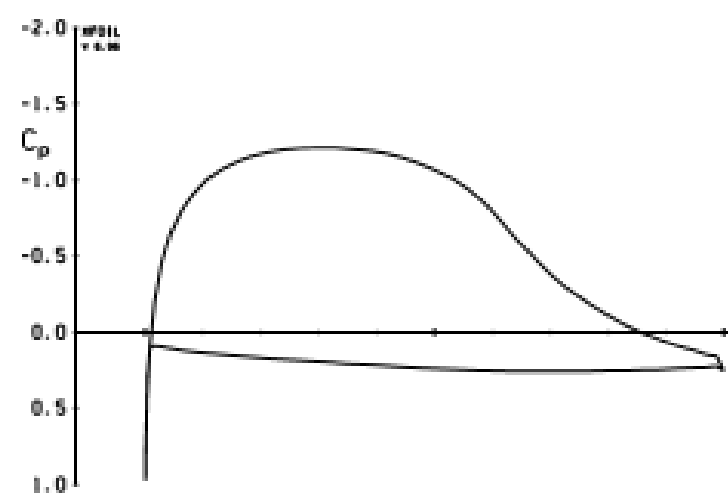
Airfoil with a circular arc camber line with radius R and zero thickness. p_u is the upper surface pressure, p_l is the lower surface pressure.

Problem 1. Reflected airfoil



For the airfoil shown above, carefully sketch the pressure distribution for $C_l = 0.4$ assuming an incompressible potential flow. Also, assume that the airfoil has been designed so that, at this lift coefficient, there is no suction peak at the leading edge.

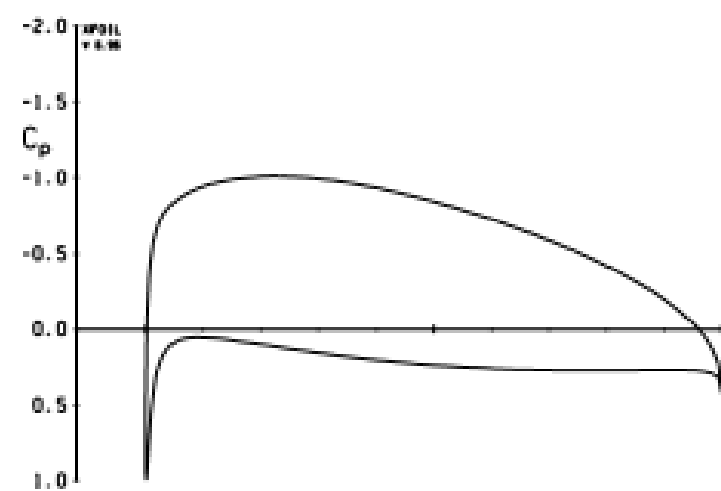
Problem 3. Local pressure around an airfoil



Distribution 1



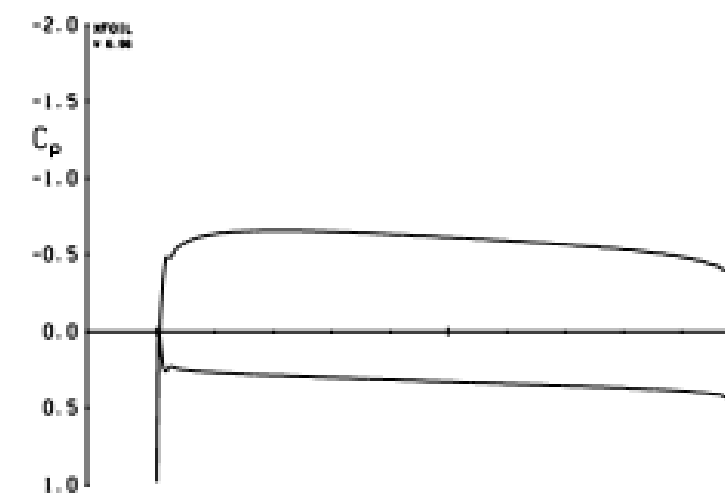
Airfoil A



Distribution 2



Airfoil B



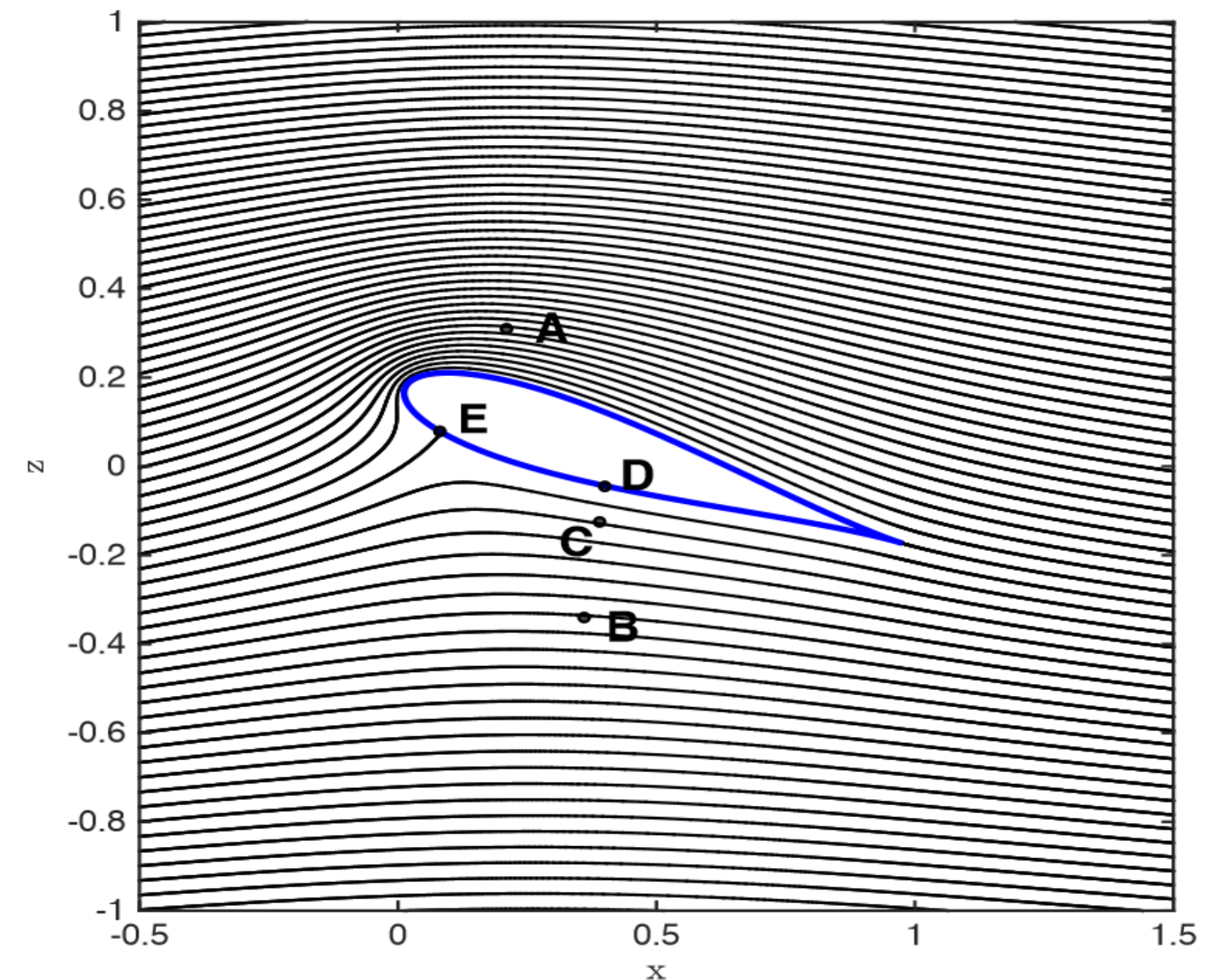
Distribution 3



Airfoil C

Three airfoil geometries and the pressure distributions for these airfoils are shown for an incompressible, inviscid flow with a lift coefficient of 0.9. Relate the airfoil geometries with the pressure distributions.

Problem 3. Local pressure around an airfoil

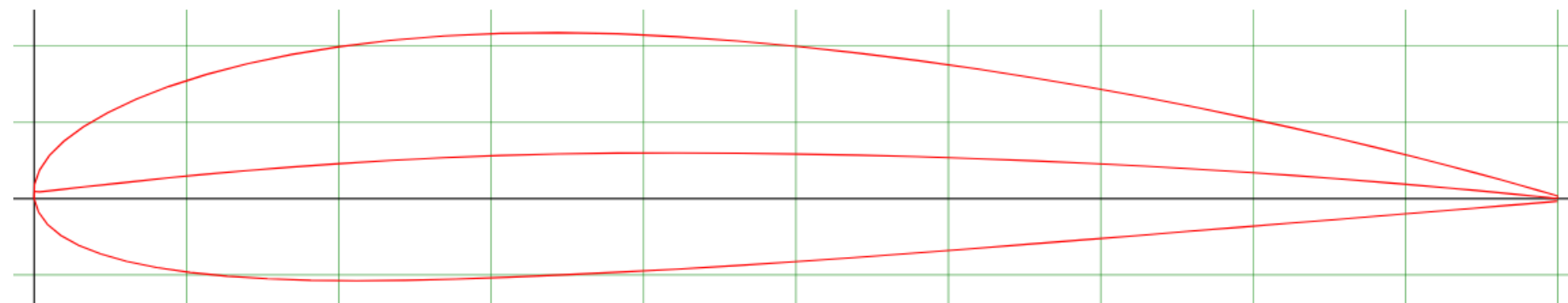


The streamlines for the steady, inviscid, and incompressible flow around a symmetric airfoil at an angle of attack are shown in the above figure. The flow in the freestream (far upstream of the airfoil) has uniform velocity \vec{V} and uniform pressure p_∞ . The density is ρ . How do the pressures at the labeled points relate to p_∞ ?

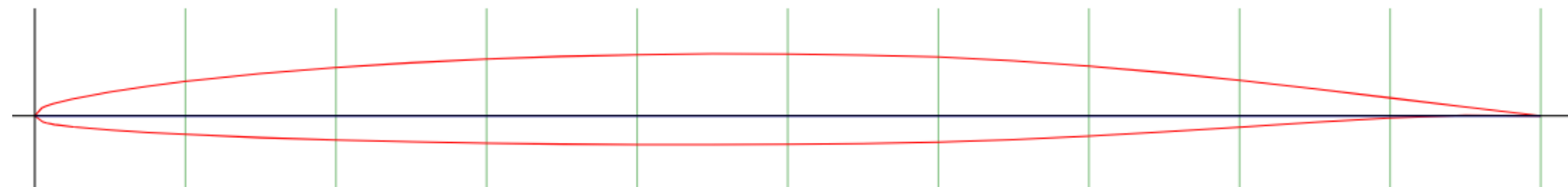
Problem 4. Four airfoils

Match the four airfoils to the following types of aircraft and explain your reasoning:

- Micro Unmanned Aerial Vehicle
- General Aviation Aircraft
- Transonic transport
- Supersonic aircraft

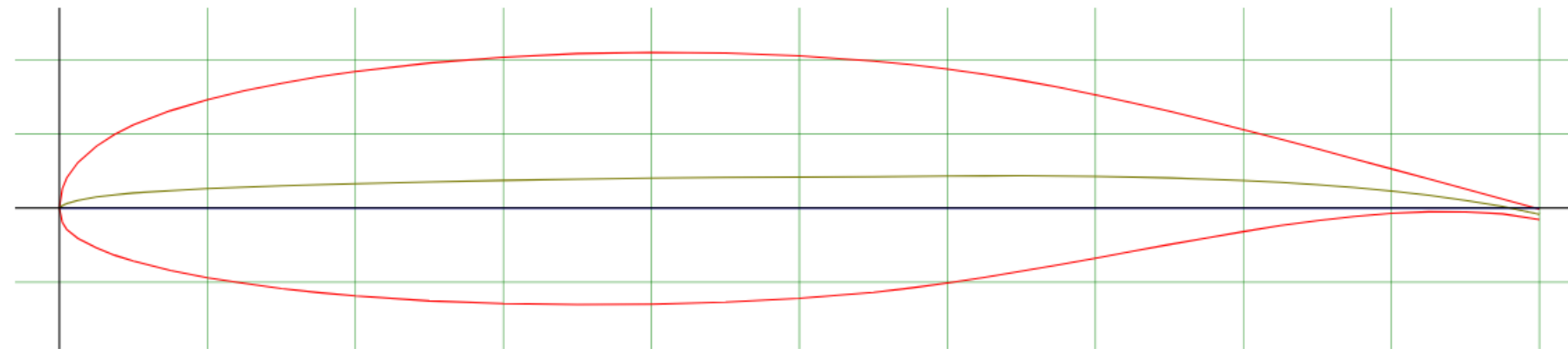


NACA 3416



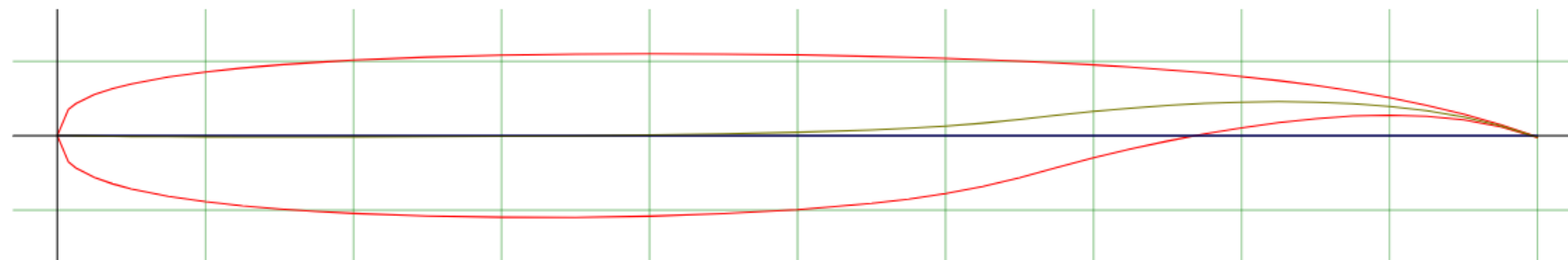
NACA 66-206

NACA 66-206 airfoil
Max thickness 6% at 45% chord
Max camber 1.1% at 50% chord



NASA/LANGLEY LS(1)-0417 (GA(W)-1) AIRFOIL

Max thickness 17% at 40% chord.
Max camber 2.4% at 65% chord.



WHITCOMB INTEGRAL SUPERCritical AIRFOIL

Max thickness 11% at 35% chord.
Max camber 2.4% at 82.5% chord.